Journal of Medicinal Chemistry

Article

Identification of a New Zinc Binding Chemotype by Fragment Screening

Panagiotis K. Chrysanthopoulos, Prashant Mujumdar, Lucy A. Woods, Olan Dolezal, Bin Ren, Thomas S. Peat, and Sally-Ann Poulsen

J. Med. Chem., **Just Accepted Manuscript** • DOI: 10.1021/acs.jmedchem.7b00606 • Publication Date (Web): 17 Aug 2017

Identification of a New Zinc Binding Chemotype by Fragment Screening

Panagiotis K. Chrysanthopoulos[1,#], Prashant Mujumdar[1,#], Lucy A. Woods[1], Olan Dolezal[2], Bin Ren[2], Thomas S. Peat[2,*] and Sally-Ann Poulsen[1,*]

[1]Griffith University, Griffith Institute for Drug Discovery, Nathan, Brisbane, Queensland 4111, Australia

[2]CSIRO, Biomedical Manufacturing Program, 343 Royal Parade, Parkville, Melbourne, Victoria 3052, Australia

[#]Equal first authors

Email s.poulsen@griffith.edu.au, tom.peat@csiro.au

Abstract

The discovery of a new zinc binding chemotype from screening a non-biased fragment library is reported. Using the orthogonal fragment screening methods of native state mass spectrometry and surface plasmon resonance a 3-unsubstituted-2,4-oxazolidinedione fragment was found to have low micromolar binding affinity to the zinc metalloenzyme carbonic anhydrase II (CA II). This affinity approached that of fragment sized primary benzene sulfonamides, the classical zinc binding group found in most CA II inhibitors. Protein X-ray crystallography established that 3-unsubstituted-2,4-oxazolidinediones bound to CA II via an interaction of the acidic ring nitrogen with the CA II active site zinc, as well as a hydrogen bond between the oxazolidinedione ring oxygen and the CA II protein backbone. Furthermore, 3-unsubstituted-2,4-oxazolidinediones appear to be a viable starting point for the development of an alternative class of CA inhibitor, wherein the medicinal chemistry pedigree of primary sulfonamides has dominated for several decades.

Introduction

Proteins that require a metal cofactor for function have gained significant traction as therapeutic targets,[1, 2] with the mechanism of action of a number of clinically approved drugs and investigational compounds attributed to metalloenzyme inhibition.[3-6] Zinc is one of the most abundant metal cofactors in the human proteome[7, 8] and small molecule zinc metalloenzyme inhibitors usually comprise a zinc binding pharmacophore[9] that interacts directly with the metal ion to block endogenous activity.[10-12] The importance of zinc proteins is exemplified in recent studies that show a correlation between zinc recruitment and the complexity of eukaryotic genomes.[13] There are a number of zinc binding groups (ZBGs) that have been explored in exquisite structural detail for binding to zinc metalloenzymes, these include the carboxylate, hydroxamate, sulfonamide, thiol and phosphonate functional groups. These functional groups are well represented in the ligands of zinc metalloprotein-ligand structures that have been deposited with the protein data bank (PDB) and in approved drugs targeting metalloenzymes.[14] With the advent of fragment based drug discovery (FBDD) has come a new opportunity to discover alternate and novel metal binding groups by fragment screening.[15] Fragment screening represents a dramatic change in the approach to drug discovery that makes use of low molecular weight small molecules (i.e. fragments) for unbiased identification of novel structural motifs that bind to proteins with high ligand efficiency. A hit fragment may be structurally elaborated to a new chemical entity with drug-like properties and functionality to improve strength and specificity of binding interactions with the target protein. Since 2005, fragment screening has resulted in more than 30 drug candidates that have entered clinical trials, with two U.S. Food and Drug Administration (FDA) approved drugs and several more compounds in advanced trials.[16] The relatively short timeframe from fragment to U.S. FDA approved drugs has led to adoption of fragment screening approaches in academia, biotech and pharma.[16] A combination of FBDD with

metalloprotein targets has been the focus of several successful FBDD campaigns by Cohen and colleagues utilising fragment libraries assembled from pharmacophores that have a known predilection toward metal binding.[12, 17, 18] Additionally, Klebe and colleagues have characterised the structure of a number of alternate ZBGs for carbonic anhydrase II (CA II, EC 4.2.1.1).[19]

Our group is interested in modulating carbonic anhydrase (CA) activity for therapeutic purposes and has previously targeted inhibition of this zinc metalloenzyme using both standard and novel medicinal chemistry strategies.[20-24] hCAs (h = human) regulate pH homeostasis by catalysing the reversible hydration of carbon dioxide to bicarbonate and a proton: $CO_2 + H_2O \leftrightarrows HCO_3^- + H^+$ and evidence is mounting that modulating tumour cell pH homeostasis may prove an effective anti-tumour strategy.[24-26] The CA active site zinc coordinates to the imidazole sidechain of three histidine residues and to the H_2O molecule involved in the CO_2 hydration reaction, hence the implied target of small molecule CA inhibitors is the CA active site zinc. A key focus of our novel CA targeting strategies has been the discovery of new chemical entities as these are critical for the drug discovery pipeline to deliver new CA-based therapeutics.[27] We recently reported two novel sulfonamide compounds, the natural product Psammaplin C (**1**)[28] and the saccharin glycoconjugate (**2**),[22] as potent, isozyme selective inhibitors of CAs, Figure 1A.

More recently we reported the findings of an unbiased fragment screening campaign with a 720-member fragment library against CA II.[29] Seven hits (**3-9**) were identified, including known ZBGs such as a primary sulfonamide (**3**) and carboxylates (**4-6**), Figure 1B.[29-33] More interesting however was the finding of two 5-substituted tetrazoles (**7** and **8**) and a 3-substituted-1,2,4-triazole (**9**) as hits, Figure 1B. Compounds **7-9** are not classic acidic

functional groups like carboxylates and sulfonamides, but instead may be considered as acidic heterocycles. Additionally these heterocycles were not previously known as CA II binding chemotypes, ZBGs or metal binding groups generally. The strong binding affinity of the primary sulfonamide functional group for CA II compared to other known ZBGs is attributed to two key hydrogen bonds with the active site threonine residue, that are in addition to the zinc-sulfonamide interaction, Figure 2. The specificity of the two key hydrogen bonds ensures that the sulfonamide ZBG has very high selectivity for CA with minimal binding to other zinc metalloenzymes.[34]

In this manuscript we disclose the discovery of an additional fragment hit (compound **10**) against CA II that was detected from the same 720-member unbiased fragment library, bringing the total number of hits to eight, a hit rate of 1.1%. Compound **10** is a 3-unsubstituted-2,4-oxazolidinedione. This chemotype was not previously known for zinc binding, however compound **10** exhibited particularly strong binding affinity for CA II (K_D = 3.5 μM). This affinity approaches that of the classical primary sulfonamide ZBG of CA inhibitors such as **3** (K_D = 1.4 μM), and far exceeds the CA II affinity for compounds **4-9** (K_Ds 631 - 1280 μM). To define the structural basis and boundaries for the observed strong binding to CA, we investigated the detailed structure-activity relationship (SAR) for the oxazolidinedione chemotype. Our approach to generate SAR employs a combination of chemical design and synthesis to prepare fragment analogues, followed by biophysical characterisation of the new fragment analogues with native state mass spectrometry (MS), surface plasmon resonance (SPR) and protein X-ray crystallography (XRC). Furthermore, we have utilised MS for qualitative, semi-quantitative and quantitative fragment screening to evaluate fragment SAR, known as "SAR by MS".[35] The discovery of the 3-unsubstituted-2,4-oxazolidinedione chemotype as a new ZBG contributes to the growing importance of small

molecule CA inhibitors that comprise non-classical features, as well as alternate and novel ZBGs for drug development generally.

A.

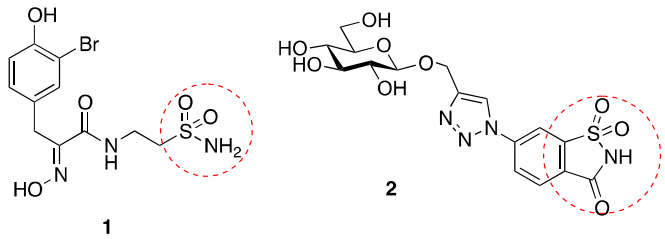

B.

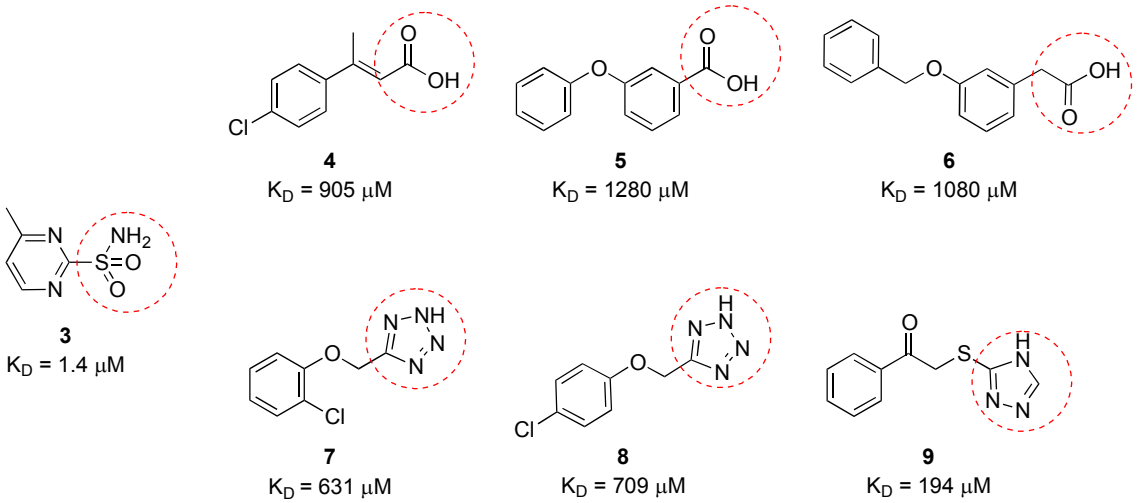

Figure 1. A) Unusual carbonic anhydrase (CA) inhibitors Psammaplin C (**1**)[28] and saccharin glycoconjugate (**2**)[22]. B) Fragment hits (**3-9**) identified from an unbiased fragment screening campaign of the CSIRO fragment library targeting CA II.[29] The known or probable zinc binding group of each fragment is circled.

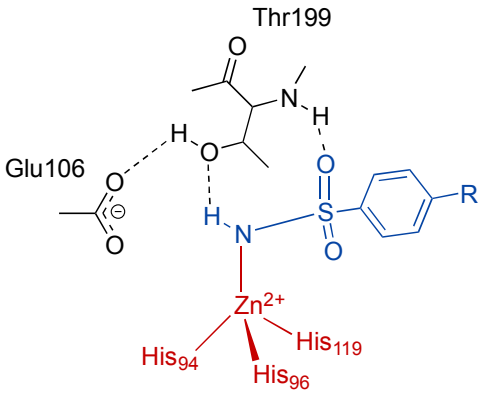

Figure 2. Common binding pose observed for >200 primary sulfonamide:CA II complexes reported in the Protein Data Bank.[36]

Results and Discussion

1-Phenyl-2,4-oxazolidinedione **10** was identified and validated as a binder for hCA II by fragment screening of a non-biased synthetic fragment library using orthogonal fragment screening techniques: SPR and native state mass spectrometry, Figure 3A. The binding affinity (K_D) of **10** for hCA II is 3.5 μM (ligand efficiency = 0.57), as determined by SPR. This affinity is similar to that of the sulfonamide fragment **3** (K_D = 1.4 μM, ligand efficiency = 0.73) but 2-3 orders of magnitude stronger than that for the non-sulfonamide fragments **4-9** (K_D range 631 - 1280 μM).[29, 36a] We were keen to investigate the structural basis of the strong binding and ligand efficiency of **10** to hCA II and to establish if the 3-unsubstituted-2,4-oxazolidinedione heterocycle is a viable starting point for the development of a new class of CA inhibitor to rival the classic primary sulfonamide chemotype, wherein the medicinal chemistry pedigree has already spanned several decades. Computed physicochemical descriptors, absorption, distribution, metabolism and excretion parameters, pharmacokinetic properties, drug-like nature and medicinal chemistry friendliness of benzene sulfonamide and compound **10** indicate that 3-unsubstituted-2,4-oxazolidinedione is a developable fragment

for drug discovery (supporting information, Figure S20 and S21).[36b] We determined the protein X-ray crystal structure of fragment **10** bound to hCA II, Figure 3B. The fragment bound via an interaction of the acidic ring nitrogen with the hCA II active site zinc. The pK_a value for the -NH- of **10** (pK_a of 5.5) together with the pK_a values of a series of phenyl and benzyl substituted five membered heterocycles predicted to be acidic bioisosteres were measured more than 25 years ago to acquire data for the calculated Log P (cLog P) database, Pomona College MedChem CLOGP.[37] The hCA II:**10** structure is consistent with the prediction that 3-unsubstituted-2,4-oxazolidinedione is an acidic bioisostere.[37] In addition to the zinc binding interaction there are two hydrogen bonds between the fragment heteroatoms and hCA II. A hydrogen bond (3.0 Å) is formed between the ring –O– of **10** with the Thr199 backbone nitrogen, while a second hydrogen bond is formed with the ring –N– of **10** and Thr199 side chain hydroxyl (3.2 Å). These interactions are akin to the primary sulfonamide binding pose, and likely account for the comparable binding affinity to sulfonamides and the increased binding affinity over fragments **4-9**, Figure 4. Compound **10** is a very efficient fragment as each of its four heteroatoms contribute to hCA II binding – either by direct interactions or by imparting increased acidity on the imide nitrogen. A related compound, 1-(2′,4′-dimethoxyphenyl)-2,4-oxazolidinedione **11**, was obtained from the CSIRO compound collection. Compound **11** has a comparable K_D (6.1 μM) to **10** and bound to hCA II similarly via interaction with zinc, and two H-bonds to Thr199, Figure 3B.

We next searched the PDB against the 3-unsubstituted-2,4-oxazolidinedione fragment and identified only one protein:ligand crystal structure where the ligand comprises this fragment, the ligand is (5*R*)-5-(3-{[3-(5-methoxybenzisoxazol-3-yl)benzimidazol-1-yl] methyl}phenyl)-5-methyloxazolidinedione (**12**, Figure 3A) in complex with the peroxisome proliferator-activated receptor γ subtype (γPPAR).[38] γPPAR is involved in regulating glucose

metabolism and insulin sensitivity, and γPPAR modulation has potential for development of treatment of type 2 diabetes mellitus.[38] The oxazolidinedione moiety of **12** was incorporated as a replacement for a phenoxycarboxylic acid group of a lead compound series. The structure of the γPPAR:**12** complex (PDB ID 3TY0) indicates there are hydrogen bond interactions of the oxazolidinedione to the Ser342 backbone nitrogen and the His266 side chain nitrogen of γPPAR. Notably γPPAR is not a metalloprotein hence there is no opportunity for a metal binding interaction in this protein.[38] The finding that **10** and **11** bind to the hCA II active site zinc, coupled with the lack of exemplar 3-unsubstituted-2,4-oxazolidinediones as a ZBG in the PDB, establishes the 3-unsubstituted-2,4-oxazolidinedione as a new zinc binding chemotype.

A.

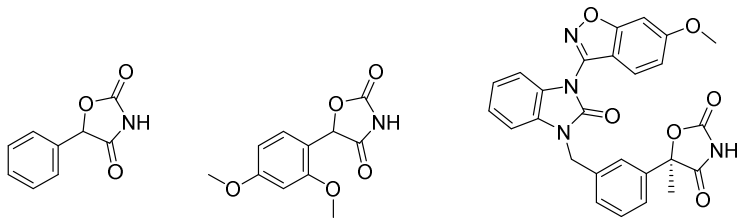

10 **11** **12**

B.

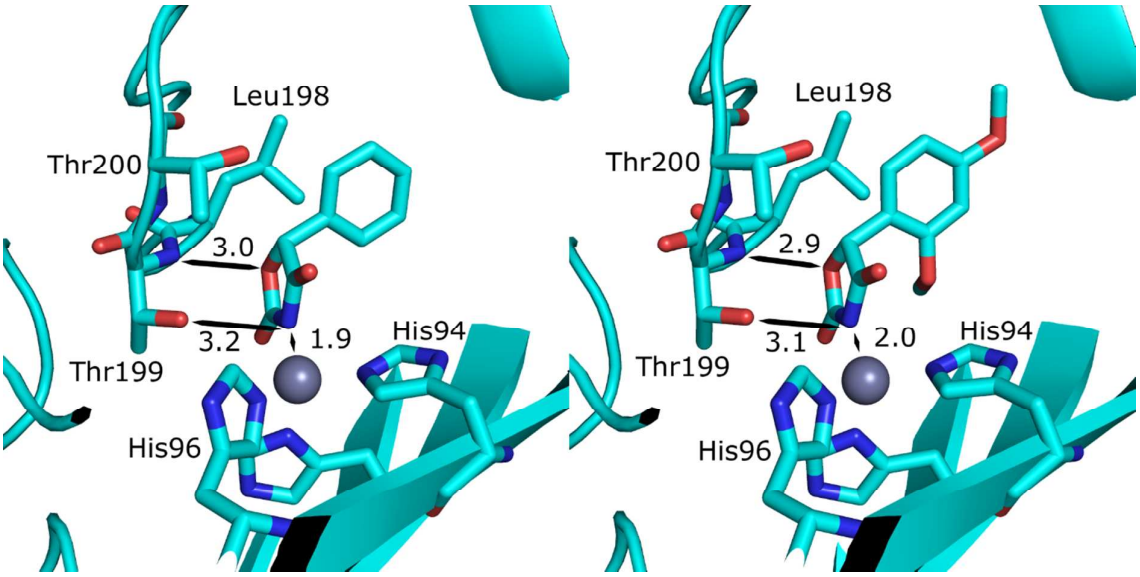

Figure 3. (A) 3-Unsubstituted-2,4-oxazolidinediones **10**, **11** (this study) and γPPAR inhibitor **12**.[38] (B) Crystal structures of **10** and **11** with carbonic anhydrase II (CA II). In panel A, **10** is shown in the crystal structure with the zinc atom represented by a grey sphere and active site residues labelled (His94, His96, Leu198, Thr199, Thr200; His119 is underneath the zinc atom). Distances from the protein to the compound are shown in Angstroms. In panel B, **11** is shown in approximately the same orientation as **10**, with the same active site residues labelled as in panel A.

A. B.

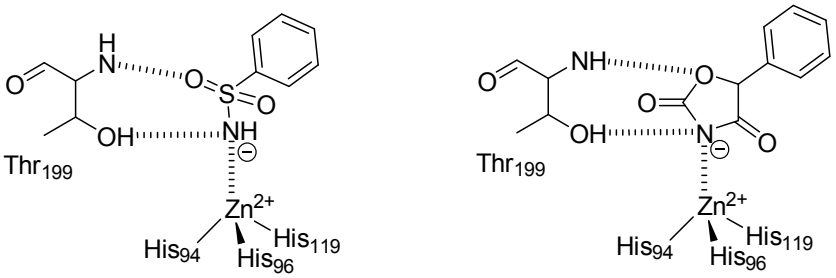

Figure 4. Binding interactions of the classic primary sulfonamide chemotype (A) with CA II are emulated by the oxazolidindione chemotype (B), discovered by fragment screening.

Compound design to establish SAR

To ascertain the structure-activity relationships (SAR) for binding of the oxazolidinedione fragment to CAs, a series of structural modifications were made to the heteroatoms and to the 5-substituent with the acidic cyclic imide NH group retained in all compounds. The SAR focussed library comprised lead compounds **10** and **11** (Figure 3) and new compounds, **13** – **29**, Figure 5. Specifically, the replacement of the ring heteroatom from –O– (oxazolidinediones, **10** and **11**) to either a –S– (thiazolidinediones, **13**, **16** and **17**) or–NH– (hydantoins, **15**, **18**, **19**, **20** and **21**) was examined to determine the effect of both hydrogen bond acceptor strength (–O– versus –S–) and modification of a hydrogen bond acceptor to a hydrogen bond donor (–O– and –S– versus –NH–), noting the key role of the ring oxygen in the **10**:CA II and **11**:CA II crystal structures as a hydrogen bond acceptor (2.9-3.0 Å to Thr199N). We also modified both the ring heteroatom from –O– to –NH– (hydrogen bond acceptor to hydrogen bond donor) together with one of the carbonyls to a thiocarbonyl (thiohydantoins, **26** and **27**). Depending on ease of synthesis, these heteroatom changes were combined with modification of the 5-substituent (phenyl, benzyl or benzylidene derivatives) with or without added methoxy electron withdrawing groups. Additionally, the replacement of both the –O– heteroatom and the 4-carbonyl oxygen with sulfur atoms denotes the 2-thioxo-1,3-oxazolidin-4-one (**14**) and rhodanine heterocycle (rhodanines, **22**, **23**, **24** and **25**), which have further altered hydrogen bonding capacity compared to **10** and **11**. To the best of our knowledge none of these chemotypes have been tested for binding to or inhibition of CAs. Finally, we included two FDA approved fragment-sized oxazolidinediones, the anticonvulsant trimethadione **28** and its demethylated metabolite dimethadione **29**, Figure 5,

in this focussed library. The final assembled library comprised 19 compounds (**10**, **11**, **13** – **29**) of molecular weight <300 Da.

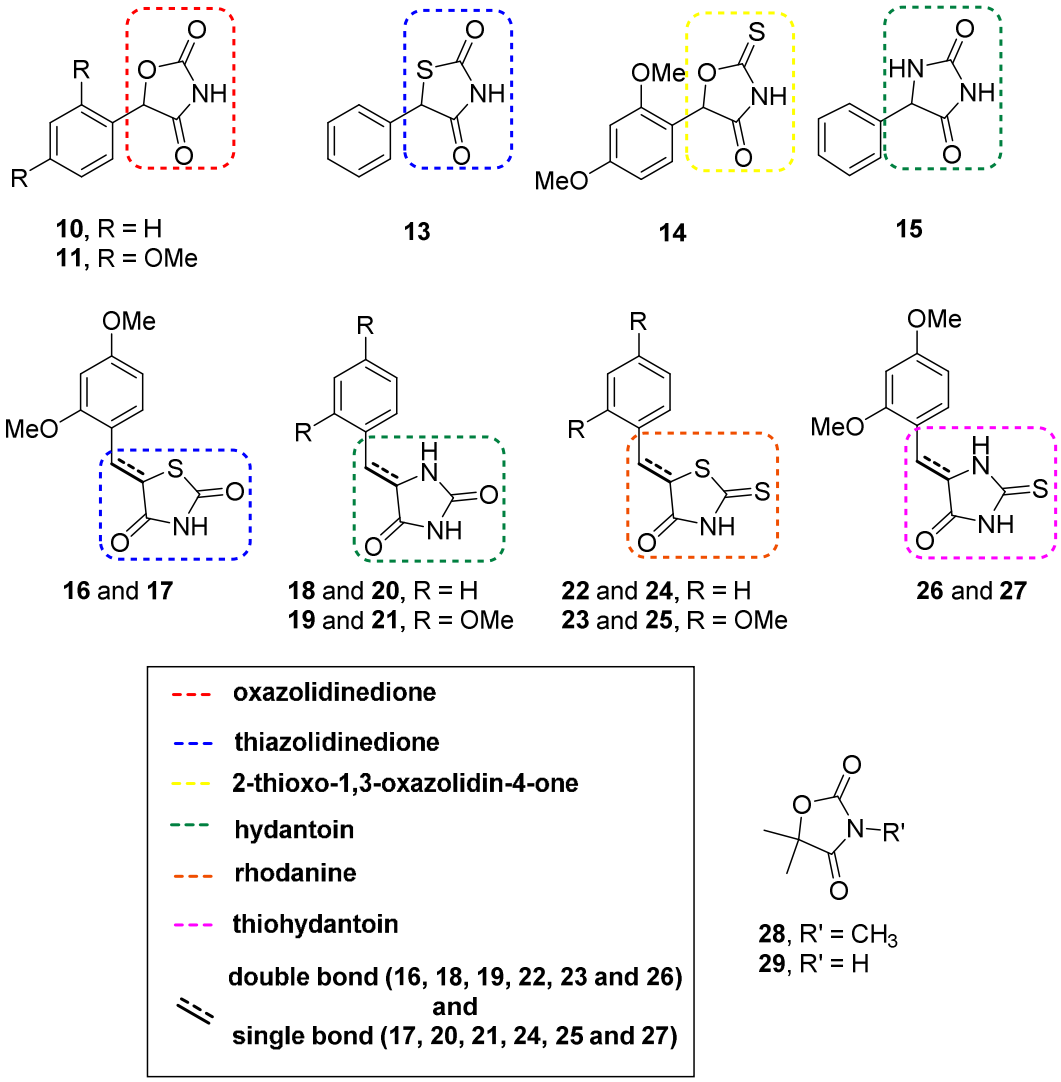

Figure 5. Focussed fragment library to establish SAR around the oxazolidinedione ZBG chemotype (**10** and **11**) for CA affinity.

Compound Screening

Screening of the focussed fragment library **13**–**29** and lead hit fragments **10** and **11**, was carried out first using native state mass spectrometry, followed by SPR for validation. X-ray crystallography was employed to provide a detailed analysis of protein-fragment interactions for validated hits.

Nanoelectrospray ionisation (nanoESI) mass spectra were acquired with test samples comprising CA II with one equivalent of added compound (**10**, **11**, **13** – **29**). Nine compounds were observed bound to CA II - **10**, **11**, **13**, **14**, **17**, **22**, **24**, **25** and **27**. The observation of [protein + fragment] complex in the nanoESI mass spectrum enables qualitative classification of a fragment as a hit (or "binder") or non-hit (or "non-binder"), with arbitrary thresholds possible to further delineate fragment binding as strong, medium or weak. Native state mass spectrometry has been applied to the study of noncovalent protein-ligand interactions for the measurement of K_D values,[39, 40] there are however few examples of mass spectrometry for fragment screening,[29, 41-45] and mass spectrometry is not yet fully evaluated as a primary fragment screening method. To incorporate quantification to the nanoESI method we introduce here the concept of mass spectrometry fragment binding (FB_{MS}), specifically we assess the potential of the FB_{MS} metric to quickly and accurately quantify the relative binding strength from mass spectrometry data. FB_{MS} is expressed as a percentage and is determined from the fraction of the intensity of the [protein + fragment] peaks relative to total protein peaks, Equation 1, where $I_{[P:F]}$ and $I_{[P]}$ are the mass spectrometric peak intensities of the [protein + fragment] complexes and free/acetate bound protein, respectively, in the ESI mass spectrum at a specified protein and fragment concentration. FB_{MS} values for CA II and fragment, when equimolar amounts of protein and fragment (7.5 μM each) are analysed, are in Table 1 (columns 3 and 4).

$$FB_{MS} = \frac{I_{[P:F]}}{I_{[P:F]}+I_{[P]}} \times 100\% \qquad \text{Equation 1.}$$

Next K_D values were determined for eight of the hit fragments (insufficient sample of **14** available at time of experiment). Experiments were performed with CA II (14.5 μM) titrated against at least five different fragment concentrations ([F] range 0.5 μM - 120 μM) until either full complexation was observed (i.e. $I_{[..]} = 0$) or the fragment concentration reached 120 μM. The FB_{MS} was calculated for each fragment concentration and values plotted against fragment concentration [F]. The K_D was calculated upon curve fitting this plot based on Hill slope analysis, Figure 6.[46] K_Ds ranged from 2.3-50.7 μM, (Table 1, columns 5 and 6). All observed charge states (+9, +10 and +11) were utilised for both FB_{MS} and K_D calculations (Table 1, columns 3 and 5). Additionally for comparison, FB_{MS} and K_D calculations were performed using only the peak intensities for the +10 charge state, (Table 1, columns 4 and 6). Representative mass spectra showing the +10 charge state acquired for the CA II + **24** titration (K_D = 16.7 μM) are presented in Figure7. The single charge state (+10 only) calculated values are in excellent agreement with calculated values using all charge states (+9, +10 and +11), indicating that the single charge state calculation of FB_{MS} and K_D will be sufficient for future fragment screening campaigns using nanoESI-MS. FB_{MS} values provide a useful rank order of binding strength compared to K_D calculations determined from more laborious and higher sample consuming titration experiments, the overall trend is consistent.

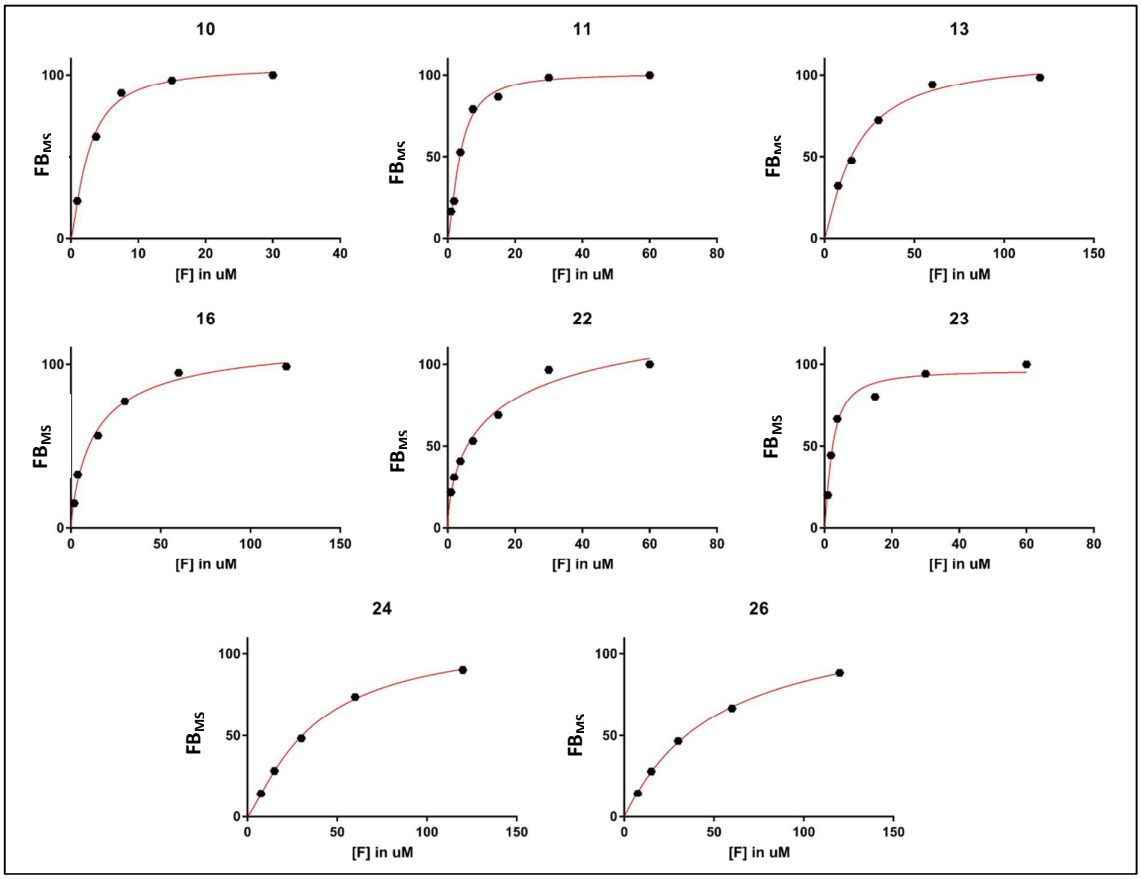

Figure 6. Saturation curves of the nanoESI-MS titration of eight hit fragments with CA II (14.5 μM). FB_{MS}, as calculated at each fragment concentration using all observed charge states (+9, +10 and +11), is plotted against total fragment concentration [F] with curve fitting based on Hill slope analysis used to determine K_D.[46]

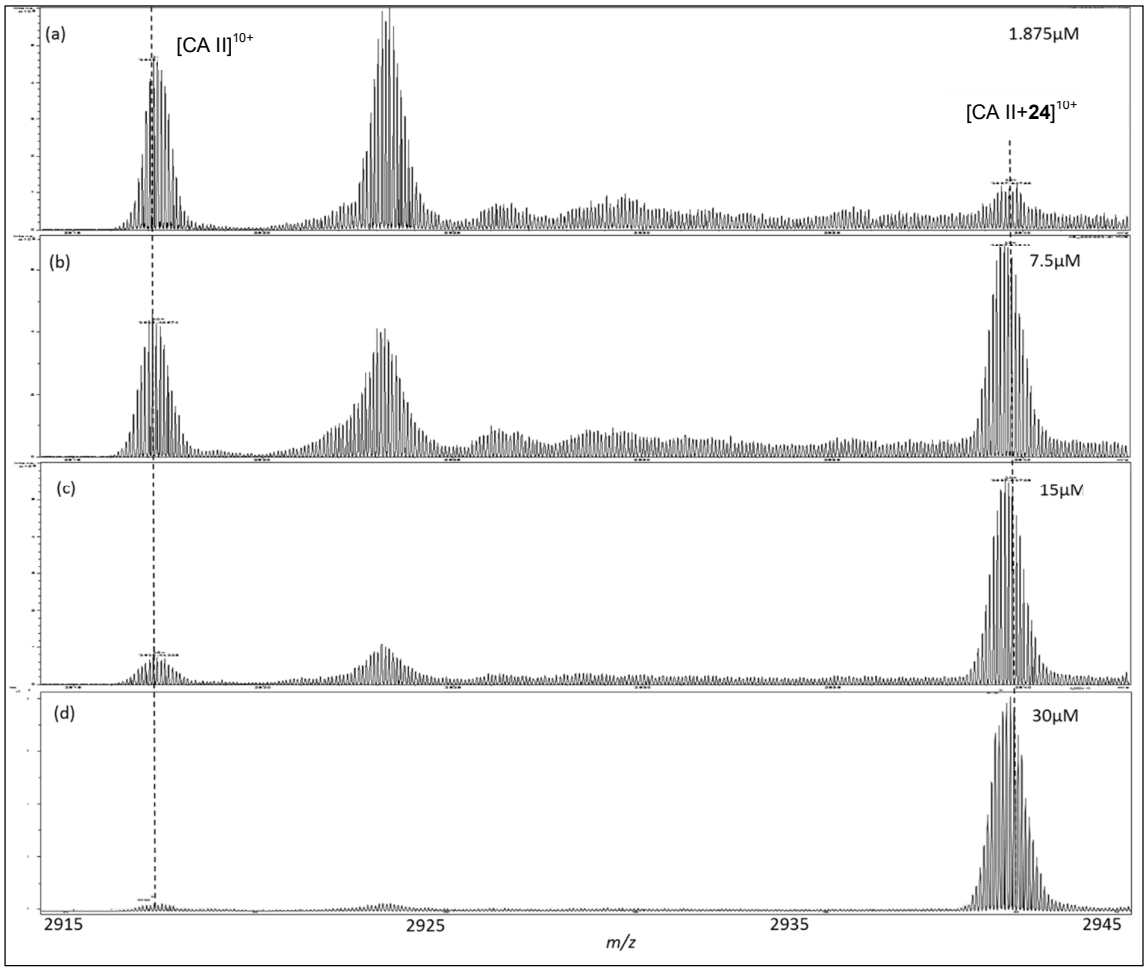

Figure 7. Representative positive ion mode nanoESI mass spectra (+10 charge state) of 14.4 μM hCA II (pH 7.4 10 mM NH_4OAc) titrated with fragment **24** to determine fragment K_D by nanoESI-MS: (a) 1.875 μM of **24**; (b) 7.5 μM of **24**; (c) 15 μM of **24**; and (d) 30 μM of **24**.

SPR was used as a secondary orthogonal fragment screening method for compounds **10**, **11** and **13**–**29**, Table 1 (column 2). Binding sensorgrams for compounds interacting with the immobilised CA II are provided in Supporting Information. SPR analysis identified the same nine compounds that bound to CA II as identified by nanoESI-MS, with K_Ds that ranged from 3.4-65.5 μM (excluding **22**), Table 1 (column 2). The K_D values calculated by the nanoESI-MS experiments are in good agreement (K_D range 2.3-50.7 μM) with the values measured in solution by SPR with two exceptions. K_D values of fragment **22** (nanoESI-MS K_D = 35.8 μM,

SPR K_D = 355 μM) differ by a factor of ten, however the K_D for **22** could not be reliably determined by SPR due to solubility issues of this compound in the SPR buffer and this issue is likely responsible for the discrepancy observed. Compound **23** was not detected by nanoESI-MS however was detected by SPR. Notably, **23** had the weakest binding of the SPR hits (K_D ~ 1000 μM), much weaker than all other hit fragments. Non-binding compounds were fully consistent using the orthogonal methods. The rank order of K_Ds by the two methods followed a similar trend: nanoESI-MS K_D values, low to high: **25**, **10**, **11**, **17**, **24**, **13**, **22**, **27/27′**; SPR K_D values, low to high: **25**, **10**, **11**, **24**, **17**, **14**, **13**, **27/27′, 22**, **23** (for details on structure of **27**/**27′** see Table 1 footnote). This is consistent with our earlier findings where we also found very good overlap with hits identified using SPR (as the primary screen) and nanoESI MS.[29] The finding that nanoESI-MS and SPR provide agreement of both the magnitude and trend of K_D values suggests that the straightforward metric FB_{MS}, with equimolar protein and fragment concentrations, offers the opportunity for rapid, semi-quantitative assessment of fragment binding strengths. If nanoESI-MS is selected as a primary screen we propose that MS has at least equal potential to other screening methods in use to accelerate and inform the initial steps of FBDD. As discussed by us earlier, limited overlap among different fragment screening approaches has been reported by Klebe and colleagues.[29, 46a] However in their study SPR was not included. Their study did assess native state ESI-MS, however using very different conditions to those employed herein.[29, 46a]

Table 1. Screening results for **10**, **11** and **13–29** using native state mass spectrometry, SPR and protein X-ray crystallography.

Compound No.	SPR K_D (μM)	ESI-MS FB_{MS} (%)[b]	ESI-MS FB_{MS} (%)[c]	ESI-MS K_D (μM)[b]	ESI-MS K_D (μM)[c]	Protein XRC[d]
10	3.5	87.7	79.8	2.6	3.0	Y
11	6.1	88.1	90.2	3.6	3.5	Y
13	32.9	91.5	93.7	17.4	18.4	Y
14	28.6	51.1	53.1	n.d.[e]	n.d.	Y
15	NSB[a]	SB	NSB	n.d.	n.d.	n.d.
16	NSB	NSB	NSB	n.d.	n.d.	n.d.
17	26.2	63.9	67.3	13.9	16.0	Y
18	NSB	NSB	NSB	n.d.	n.d.	n.d.
19	NSB	NSB	NSB	n.d.	n.d.	n.d.
20	NSB	NSB	NSB	n.d.	n.d.	n.d.
21	NSB	NSB	NSB	n.d.	n.d.	n.d.
22	355[f]	46.3	41.5	35.8	36.2	N
23	1000	NSB	NSB	n.d.	n.d.	N
24	7.7	84.4	85.5	16.7	19.0	Y
25	3.4	68.7	74.5	2.3	2.7	Y
26	NSB	NSB	NSB	n.d.	n.d.	n.d.
27/27'[h]	65.5	14.6	23.1	50.7	43.6	Y[g]
28	NSB	NSB	NSB	n.d.	n.d.	n.d.
29	NSB[a]	NSB	NSB	n.d.	n.d.	n.d.

[a]NSB = No significant binding (K_D>2000 μM); [b]equimolar amounts of protein and fragment (7.5 μM each) using all observed charge states (+9, +10 and +11); [c]equimolar amounts of protein and fragment (7.5 μM each) using only +10 charge state; [d]XRC – X-ray crystallography. [e]n.d. – not determined; [f]K_D (SPR) could not be reliably determined due to solubility issues of this compound in the SPR buffer. [g]The electron density of the fragment observed did not correlate with the structure of **27** but instead to an impurity in the sample, later identified as **27′**.

Protein X-ray Crystallography

The ten hit fragments identified from the fragment screening were subjected to X-ray crystallography following soaking with CA II crystals as described earlier (Table 1).[29] Eight fragments led to CA II:fragment structures observed by X-ray crystallography, with all of these fragments bound via interaction of the acidic imide nitrogen with the hCA II active site zinc (1.9-2.0 Å) and with the Thr199 side chain hydroxyl (3.1-3.3 Å) (Figure 8, Table 2 and Supporting Information). The electron density in the structure for **27** showed that there was an additional atom attached to C-5 of the ring with electron density consistent with either an OH or NH_2 substituent at C-5 of **27** (Figures 8H and 9). We re-examined a sample of **27** by LCMS and HRMS and this showed that the sample comprised the hydrated compound **27′** as an impurity (~5%) (Figure 9). Co-formation of C-5 benzylidine thiohydantoins with hydrated C-5 hydroxy/C-5 benzyl thiohydantoins has been reported, the addition of water to **26** instead of reduction could lead to the formation of **27′** similarly.[47] As **27′** makes two additional potential hydrogen bonds (2.6 and 2.9 Å) with CA II compared to **27**, it is plausible that the additional binding energy enables **27′** to easily outcompete **27** for the CA II binding site.

Structures for **10** and **11**, Figure 8A and 8B, were described in the introduction. For **13** and **17** (5-10-fold weaker binders than **10** and **11**), unlike the hydrogen bond formed with the ring –O– of **10** and **11** and the Thr199 backbone nitrogen, there is no corresponding hydrogen bond

formed between the ring –S– of **13** and **17** and the Thr199 backbone nitrogen, Figure 8C and 8E. For **14**, Figure 8D, the thiocarbonyl is too far away from Thr199 to make any reasonable hydrogen bonds, however the ring –O– of **14** is 3.1 Å from the backbone nitrogen of Thr199, similar to the distance seen in compounds **10** and **11** (~3.0 Å). Compounds **25** (nanoESI-MS K_D = 2.7 μM, SPR K_D = 3.4 μM) and **24** (nanoESI-MS K_D = 19 μM, SPR K_D = 7.7 μM) are relatively strong binders, but neither the ring –S– nor the thiocarbonyl of **24** or **25** make any hydrogen bond interactions with CA II, Figure 8F and 8G.

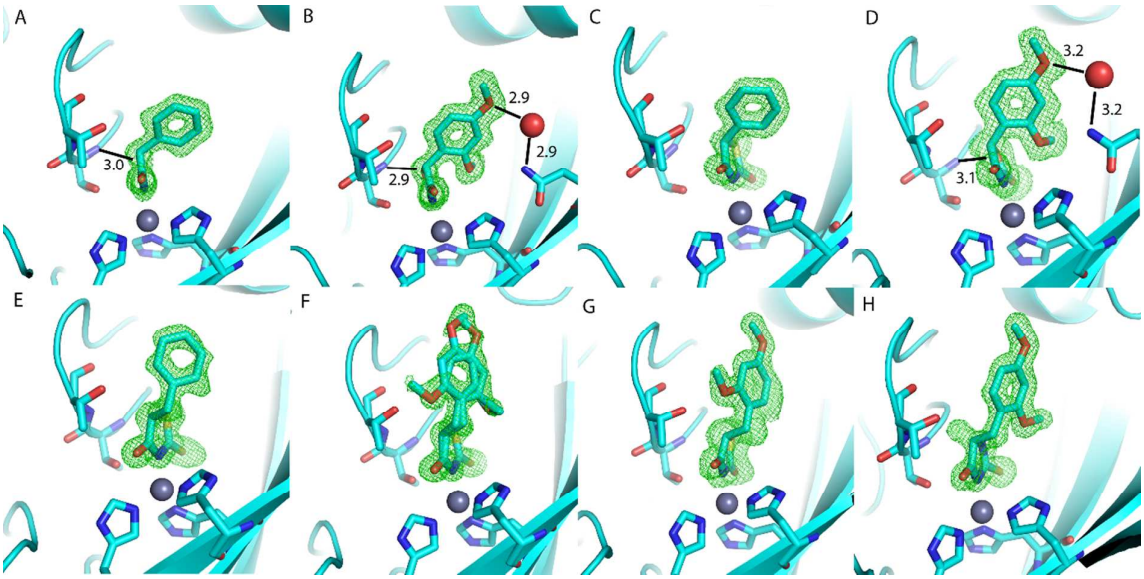

Figure 8. Difference density maps of fragments in the CA II binding site. (A) **10**, oxazolidinedione chemotype. (B) **11**, oxazolidinedione chemotype. (C) **13**, thiazolidinedione chemotype. (D) **14** 2-thioxo-1,3-oxazolidin-4-one chemotype. (E) **17**, thiazolidinedione chemotype. (F) **24**, rhodanine chemotype. (G) **25**, rhodanine chemotype. (H) **27**, thiohydantoin chemotype. Difference density (mFo-DFc) for all maps is shown at a 3σ contour level where the fragments were omitted from the model. The active site zinc atom is represented as a grey sphere. Thr199, Thr200 and the three catalytic His residues (His94, His96 and His119) are shown. There is a water molecule (red sphere) within hydrogen

bonding distance of a methoxy substituent for compounds **11** and **14** (B and D). Additionally, for compounds **10**, **11** and **14** the ring oxygen is within hydrogen bonding distance of the backbone nitrogen of Thr199 and this distance is shown (A, B and D). Also note **24** (F) is modelled in two orientations for the dimethoxyphenyl group whereas the other compounds with this group had one preferred orientation (**11**, **14**, **25** and **27′**).

Table 2. Interactions of compounds with CA II identified by protein X-ray crystallography.

Compound	**PDB ID**	**Protein-fragment interaction (Å)**				
		Zn-NH	T199OH-NH	T199N-O1 (S1)	T200NH-OH	T200OH-OH
10	5TXY and 5TY8	1.9	3.2	3.0	-	-
11	5TY9	2.0	3.1	2.9	-	-
13	5TYA	2.0	3.1	(3.7)	-	-
14	5U0D	1.9	3.3	3.1	-	-
17	5U0G	2.0	3.1	(3.6)	-	-
24	5U0E	2.0	3.2	(3.7)	-	-
25	5U0F	2.0	3.2	(3.7)	-	-
27′	5VGY	1.9	3.1	-	2.9	2.6

A.

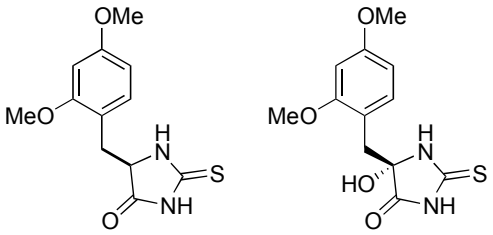

27 **27'**

B.

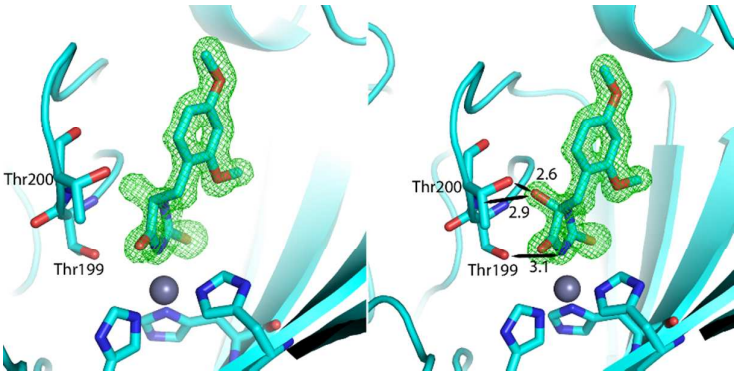

Figure 9. The electron density observed for compound **27** with CA II is consistent with an OH substituent at C-5 (**27′**). Compound **27′** was subsequently identified as a ~5% impurity in **27**. This oxygen makes two potential hydrogen bonds with the Thr200 residue: one at 2.6 Å to the sidechain hydroxyl and another at 2.9 Å to the backbone nitrogen (shown in figure).

The two compounds that failed to provide electron density in the CA II protein X-ray crystal structures were **22** and **23**. As discussed above, **23** was the weakest binding of the ten SPR hits (K_D ~ 1000 μM) and was not detected by nanoESI-MS. Compound **22** provided the only significant discrepancy in the K_D values determined by nanoESI-MS and SPR, however this compound had solubility issues at the higher concentration required for SPR analysis and this may have also affected its ability to be seen in the crystallographic studies.

Structure-Activity Relationships

The strong binding properties of **10** and **11** shown previously were confirmed in the present study (SPR K_D = 3.5 μM, nanoESI-MS K_D = 2.6 μM and SPR K_D = 6.1 μM, MS K_D = 3.6 μM, respectively). Compounds **10** and **11** have similar affinity, indicating that the two methoxy groups of the dimethoxyphenyl moiety of **11** do not significantly impact on binding even though they introduce steric bulk on to the phenyl ring (*cf.* **10**) and are electron withdrawing. Replacement of the ring –O– of **10** with –S– gave the corresponding thiazolidinedione **13**, this change resulted in a ~10-fold reduction in CA II affinity. The larger size of sulfur relative to oxygen alters the orientation of the ring in the active site; the ring –S– is positioned 3.7 Å from the backbone nitrogen of Thr199, whereas in compound **10**- the corresponding distance from the ring –O– is 3.0 Å, Table 2. Replacement of the exocyclic carbonyl of **11** with a thiocarbonyl gave **14**, this change resulted in a ~10-fold reduction on CA II affinity. While the ring oxygen of **14** is 3.1 Å from the backbone nitrogen of Thr199, similar to the corresponding interaction of compounds **10** and **11**, the thiocarbonyl of **14** is too far away from Thr199 to make any reasonable hydrogen bonds. The dimethoxybenzyl group of **17** was tolerated with one of the methoxy groups making a potential hydrogen bond with the sidechain hydroxyl of Thr200 (3.0 Å), however the more rigid dimethoxybenzylidine group in **16** resulted in loss of binding to CA II. Similarly **26** was a nonbinder, while **27′** was observed (Figure 9). The introduction of the –NH– in the ring of hydantoins (**15**, **18** - **21**) abolished binding completely. Thus, thiohydantoin and hydantoin binding was lost irrespective of most of the 5-substituents, the exception being **27′** with the added C-5 hydroxyl. This SAR suggests that a hydrogen bond acceptor in the ring 1-position (–O–) provides the additional binding affinity observed for **10** and **11**. Compounds **24** (5-benzyl substituent) and **25** (5-dimethoxybenzyl substituent) were strong binders, although the electron density shows that the –S– in the ring is too far away from Thr199 to make a hydrogen bond (3.7 Å) compared to the –O– in the ring of **10** and **11**. Compounds **22** (5-

benzylidine substituent) and **23** (5-dimethoxybenzylidine substituent) failed to give a crystal structure while the reduced binding observed by nanoESI-MS and SPR, suggests that the flexibility of the 5-substituent may be important as connection through the sp^2 hybridised carbon of the benzylidine substituents hinders hCA II binding. Rhodanine is identified as a 'PAIN' as this chemotype leads to pan-assay interference.[48] Our findings indicate that CA II is a possible off-target enzyme of 5-substituted rhodanine compounds, but that any binding is likely dependent on the nature of the 5-substituent. To the best of our knowledge, CA II as an off-target of rhodanines was not previously known. Given that CA II is a ubiquitous enzyme this finding may provide further caution on the decision to advance rhodanine compounds in medicinal chemistry campaigns. Benzylidine substitution at C5 of **16** and **26** was also poorly tolerated, while the corresponding 5-phenyl or 5-benzyl group was tolerated. This is consistent with the SAR observed for the C-5 substituent of rhodanines **22** and **23**. Finally, trimethadione **28** and dimethadione **29** have no binding to hCA II.

The SAR of the tightest binding compounds can be explained primarily by the hydrogen bonding potential of the compounds in the active site. For **10** and **11** (and to some extent, **14**), the Thr199-NH interaction with heterocycle O is a typical hydrogen bond and is the strongest interaction of the compound with the protein, other than the acidic heterocyclic nitrogen with the zinc ion (see Figure 3). The hydrogen from the backbone nitrogen of Thr199 is in the plane of the peptide bond and this is directly in line with the heterocycle oxygen (i.e. makes a 'typical' hydrogen bond interaction at this distance and angle). The heterocyclic oxygen is closer (2.9 to 3.0 Å for **11** and **10** respectively) to the Thr199 backbone nitrogen than any other part of the compound and the nitrogen hydrogen is off-centre from the middle of the heterocycle, suggesting that this could not form a pi-stacking interaction. The Thr199-OH interaction with heterocycle N presents a very different case: it is 3.1 to 3.2 Å from the acidic

nitrogen of the heterocycle and 3.9 to 4.0 Å from the zinc ion. Although the zinc ion is too far away to consider it a 'bond', it likely orients a lone pair of electrons from the hydroxyl oxygen, leaving the hydrogen to orient towards the acidic nitrogen, and this is within the typical hydrogen bonding distance. The angle for this interaction is not as good as for the Thr199-NH interaction with the heterocycle –O–, but it is still within reason. As a potential secondary interaction, one that would compete with the acidic nitrogen, the Thr199 hydroxyl sits 3.25-3.35 Å from the closest ketone/carbonyl in the hetercycle, which is long for a hydrogen bond, although the angle is not as acute, so the hydrogen could be better situated to make that interaction over the interaction to the acidic nitrogen of the heterocycle. As it is very rare to actually 'see' hydrogens in X-ray crystallography, we cannot definitively say whether the distance or angle predominates in this case (whether the hydrogen prefers to orient towards the acidic nitrogen or to the carbonyl of the heterocycle), but this will be a weak interaction in either case.

Given that the 3-unsubstituted-2,4-oxazolidinedione fragment is not known as a ZBG in the PDB, we next searched the PDB for protein:ligand crystal structures comprising the other hit fragments (as 3-unsubstituted heterocycles) to see if they are known as metal binding groups. The 2-thioxo-1,3-oxazolidin-4-one of **14** is not in the PDB. One protein:ligand crystal structure where the ligand comprises a 3-unsubstituted thiohydantoin as in **27′** is known, PDB ID 1HLF, the protein is glycogen phosphorylase B, not a metalloprotein.[49]. Three protein:rhodanine structures, with a 3-unsubstituted rhodanine, as in **24** and **25**, are known, all with the bacterial enzyme MurD ligase, also not a metalloprotein (PDB IDs 2WJP, 2Y68 and 2Y1O).[50-52] There were more than 20 protein:ligand structures in the PDB for the 3-unsubstituted 1,3-thiazolidine-2,4-diones, none of which have the fragment bound to a metal ion.[53-61]–

Interestingly, the hydantoin chemotype, although displaying no CA II binding in this study, is known as a ZBG. X-ray crystal structures of 5-substituted hydantoins with the zinc metalloenzyme, have the acidic imide nitrogen of the hydantoin coordinated to a catalytic zinc.[62-64] Further structures with matrix metalloproteins (MMP) are reported[65] showing a zinc interaction with the ligand. The zinc in these enzymes is coordinated to three protein histidine residues, the same coordination as found in hCA II. The significance of this observation is that a zinc binding group does not correspond to polypharmacology towards zinc metalloenzymes and ligand specificity is achievable when targeting metalloenzymes.

Collectively the SAR generated in this study confirms the importance of deprotonation of the acidic cyclic imide NH group for the oxazolidinedione and other heterocycles to act as a ZBG. The SAR is however more informative, it demonstrates that the zinc interaction alone is not sufficient for good CA II binding but rather that a interdependent combination of the acidic imide, a ring heteroatom (with O > S > NH, where O makes a hydrogen bond, S is neutral and the hydrogen of the N sterically interferes) and 2-carbonyl/thiocarbonyl group in parallel with the introduction of a flexible 5-substituent contribute to the strength and specificity of CA II binding. We have identified 3-unsubstituted 2,4-oxazolidinedione, 2-thioxo-1,3-oxazolidin-4-one, thiohydantoin and 1,3-thiazolidine-2,4-dione fragments as ZBGs which were not previously known in the PDB. All have potential for CA targeting strategies with new chemical entities. In contrast, the hydantoin chemotype was previously known as a ZBG yet displayed no CA II binding even though the zinc of the hydantoin binding enzymes is coordinated to three protein histidine residues, the same coordination as found in hCA II. Together the SAR of this study with the findings in the PDB indicate that strong and selective targeting of zinc metalloenzymes such as CA is possible. Notably, it is

not sufficient to have only the interaction with zinc but a combination of zinc binding with additional interactions to the protein residues is required, which then gives the ability to build in specificity.

Chemical Synthesis

The synthetic route to 2,4-oxazolidinediones **10** and **11**, 2,4-thiazolidinediones **13** and 2-thioxo-1,3-oxazolidin-4-one **14** is presented in Scheme 1. Palladium-catalysed Suzuki-Miyaura coupling reaction of the phenyl boronic acids **1a-b** with ethyl glyoxylate generated the precursor mandelic acid ethyl esters **2a-b** in good yield.[66] Condensation of **2a-b** with urea or thiourea in the presence of NaOEt (21 wt.% in ethanol), followed by acidification with HCl (1.0 N), provided the target compounds.[67]

Scheme 1. Synthesis of oxazolidindione (**10** and **11**), thiazolidinedione (**13**) and 2-thioxo-1,3-oxazolidin-4-one (**14**).

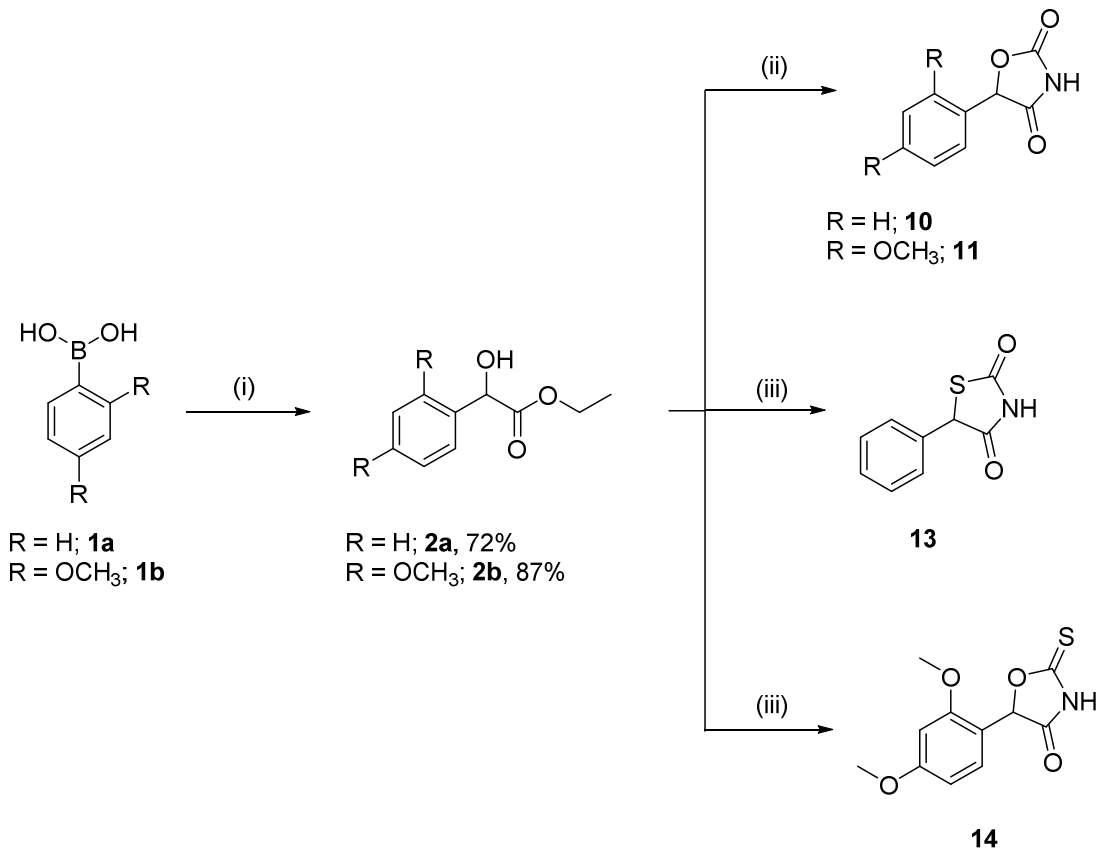

Reagents and conditions: (i) ethyl glyoxylate, $Pd_2(dba)_3.CHCl_3$, 2-(di-tert-butylphosphino)biphenyl, Cs_2CO_3, toluene 80 °C, 4-5 h; (ii) urea, 21 wt. % NaOEt in EtOH, dry EtOH, 0 °C-rt, 30 min, then reflux 3.5 h; (iii) thiourea, 21 wt. % NaOEt in EtOH, dry EtOH, 0 °C-rt 30 min, then reflux 3.5 h.

Compounds **18** and **19** were synthesised by acid mediated coupling of hydantoin with benzaldehydes **3a-b** followed by hydrolysis, Scheme 2. Reduction of the benzylidine double bond proceeded with Pd-catalysed hydrogenation to provide **20** and **21** in good yield, Scheme 2. Compound **26** was prepared similarly to **19** from **3b** and thiohydantoin, Scheme 2.[68] Attempts to reduce the benzylidine double bond of **26** with Pd/C or $Pd(OH)_2$ catalysed hydrogenation, transfer hydrogenation or 2.0 M $LiBH_4$ in THF resulted in no reaction.[68] The

reduction of **26** was however achieved with Zn-AcOH, affording benzyl thiohydantoin **27** in 65% yield (Scheme 2).[69]

Scheme 2. Synthesis of hydantoin (**18-21**) and thiohydantoin (**26** and **27**) fragments.

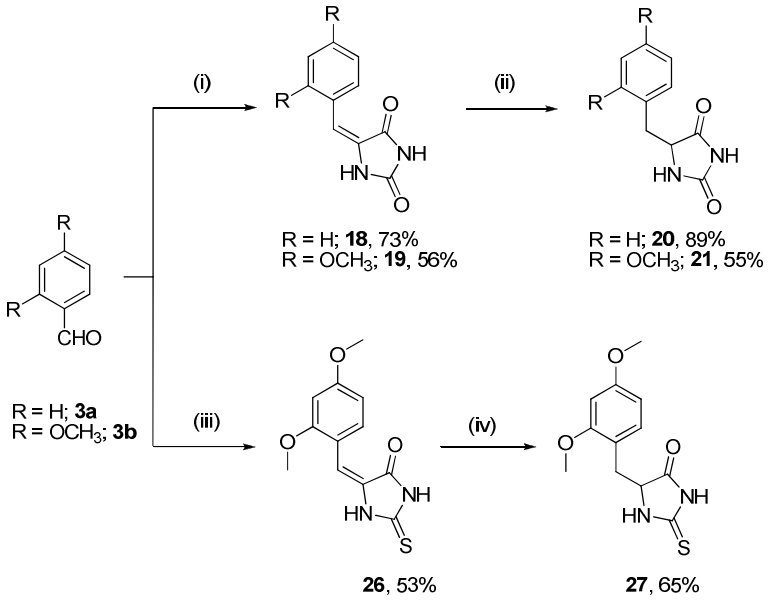

Reagents and conditions: (i) (a) hydantoin, anhyd. NaOAc, AcOH, 170 °C, 3 h; (b) H_2O, rt, overnight; (ii) 10% Pd/C, EtOH, H_2, rt, 5 h; (iii) (a) 2-thiohydantoin, anhyd. NaOAc, AcOH, 170 °C, 3 h; (b) H_2O, rt, overnight; (iv) Zn, AcOH, reflux, overnight.

Benzaldehydes **3a** and **3b** were also the core reagent for the synthesis of **16-17** and **22-25**. Knoevenagel type condensation of **3a** and **3b** with rhodanine afforded benzylidine rhodanines **22** and **23**, respectively, while reaction of **3b** and 2,4-thiazolidinedione afforded benzylidene thiazolidinedione **16**, Scheme 3.[70] Regiospecific reduction of **22**, **23** and **16** with 2.0 M $LiBH_4$ in THF provided the corresponding benzyl compounds **24**, **25** and **17**, respectively (Scheme 3).[71]

Scheme 3: Synthesis of 2,4-thiazolidinedione (**16-17**) and rhodanine (**22-25**) compounds.

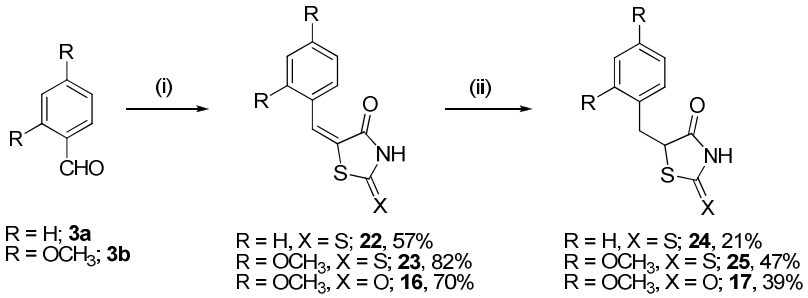

Reagents and conditions: (i) rhodanine (for **22** and **23**) or 2,4-thiazolidinedione (for **16**), NH_4OAc, toluene, reflux, 3 h; (ii) 2.0 M $LiBH_4$ in THF, pyridine-THF, reflux, 5 h; (iii) 2.0 M $LiBH_4$ in THF, pyridine-THF, reflux, 5 h.

Conclusion

Here we have discovered and assessed the CA II interactions of a new zinc binding chemotype, 3-unsubstituted-2,4-oxazolidinedione, with affinity for CA II that is of a magnitude similar to fragment sized primary benzene sulfonamides. The oxazolidinedione is an exceptionally efficient fragment for CA II. The four heteroatoms each contribute to CA II binding – either directly, by formation of two hydrogen bonds and an interaction with the active site zinc, or indirectly, by imparting acidity characteristics to the imide nitrogen. These interactions are an isostere for the classic primary sulfonamide:CA II interactions. A cascade of biophysical screening methods was employed to evaluate binding to CA II, with native state nanoESI-MS evaluated for primary screening, with SPR and protein X-ray crystallography providing validation. Our findings provide support for the relatively untapped opportunity to apply native state mass spectrometry as a complementary fragment screening method to accelerate drug discovery. Furthermore, SAR by MS[35] was employed and found to be highly suited to establish SAR around the initial hit fragment. Protein X-ray crystallography established that the 3-unsubstituted-2,4-oxazolidinedione fragment bound to

CA II via an interaction of the acidic ring nitrogen with the CA II active site zinc, as well as a hydrogen bond between the oxazolidinedione ring oxygen and the CA II protein backbone. A significant finding in relation to SAR was that hydantoins (**15**, **18-21**) had no affinity for CA II, even though the hydantoin heterocycle is known as a zinc binding chemotype with other proteins where the zinc is coordinated to three histidine residues, the same coordination as found in hCA II.[63-65] Together these finding further demonstrate that the fragment-zinc interaction alone is not sufficient for strong hCA II binding and that further hydrogen bond interactions between the fragment and hCA II are critical. This also indicates that hCA II may be selectively targeted by oxazolidinediones over other zinc metalloenzymes, consistent with the findings of hCA II binding of the classical primary sulfonamides[9] where the strong binding affinity and specificity of the primary sulfonamide functional group for hCA II is attributed to two key hydrogen bonds with the hCA II active site residues in addition to the zinc-sulfonamide interaction.[34] To conclude, 3-unsubstituted-2,4-oxazolidinedione, and other heterocycles presented herein, represent new and potentially useful starting points for development of novel and selective CA inhibitors. Additionally, native state mass spectrometry was successfully applied as a primary screen, with successful extension to generate quantitative data and SAR using "fragment SAR by MS".

Experimental

General Chemistry. All reactions were carried out in dry solvents under anhydrous conditions, unless otherwise mentioned. All chemicals were purchased commercially and used without further purification. All reactions were monitored by TLC using silica plates with visualisation of product bands by UV fluorescence (λ = 254 nm) and charring with Vanillin (6 g vanillin in 100 mL of EtOH containing 1% (v/v) concentrated sulfuric acid) stain. Silica gel flash chromatography was performed using silica gel 60 Å (230-400 mesh).

NMR (^{1}H, ^{13}C, COSY, HSQC) spectra were recorded on the 500 MHz spectrometer at 25°C. Chemical shifts for ^{1}H and ^{13}C NMR obtained in DMSO-d_6 are reported in ppm relative to residual solvent proton (δ = 2.50 ppm) and carbon (δ = 39.5 ppm) signals respectively. Multiplicity is indicated as follows: s (singlet), d (doublet), t (triplet), q (quartet), m (multiplet), dd (doublet of doublet), bs (broad signal). Coupling constants are reported in hertz (Hz). High- and low-resolution mass spectra were acquired using electrospray as the ionization technique in positive-ion and/or negative-ion modes as stated. All MS analysis samples were prepared as solutions in methanol. Purity of compounds all compounds was >95% as determined by HPLC instrument (Agilent 1100 series) with UV detection. The melting points are uncorrected. Proton and carbon atoms for NMR assignments are designated as shown in the Supporting Information.

General procedure 1: Suzuki-Miyaura coupling reaction to prepare mandelic esters.

To the appropriate boronic acid **1a** or **1b** (1.5 equiv) and Cs_2CO_3 (1 equiv) suspended in dry toulene at room temperature was added $Pd_2(dba)_3.CHCl_3$ (0.0125 equiv), 2-di-*tert*-butylphoshphanylbiphenyl (0.05 equiv) and ethyl glyoxylate (1.0 equiv) under argon atmosphere. The reaction mixture was stirred at 80 °C for 4-5 h. After completion of reaction (as evidenced by TLC), the reaction was quenched by addition of water (10-15 mL) and extracted with DCM (3 × 20 mL). The combined organic extracts were washed with brine (1 × 15 mL), dried over $MgSO_4$ and concentrated in vacuo. The crude residue was purified by flash chromatography to provide mandelic esters **2a** and **2b**, respectively.

General procedure 2: Synthesis of phenyl-2,4-oxazolidindione and phenyl-2,4-thiazolidinedione fragments.

A sodium ethoxide solution (21 wt. % in ethanol, 1.2 equiv) was cooled to 0 °C and urea (for phenyl-2,4-oxazolidindiones) or thiourea (for phenyl-2,4-thiazolidinediones) added (1 equiv) in one portion followed by dropwise addition of an ice-cold solution of mandelic ester (**2a** or **2b**, 1 equiv) in absolute EtOH (2-3 mL) over 5 min. The reaction mixture was allowed to warm to room temperature over 15-20 min and then refluxed for 3.5 h. EtOH was evaporated under vacuum, the remaining residue was suspended in a mixture of water (6 mL) and Et_2O (4 mL), acidified with 1N HCl (to pH 2-4) and extracted with Et_2O (2 × 15 mL). The combined organic extracts were washed with brine (1 × 10 mL), dried over $MgSO_4$ and concentrated in vacuo. The crude residue was purified by flash chromatography to provide compounds **10-11**, **13** and **14**.

General procedure 3: Synthesis of hydantoin and thiohydantoin fragments

Hydantoin (1.1 equiv) was added to a solution of glacial acetic acid (0.33 mL/mmol) and acetic anhydride (0.044 mL/mmol) under argon atmosphere, followed by addition of anhydrous NaOAc (2 equiv), and benzaldehyde **3a** or **3b** (1 equiv). The resulting mixture was stirred at 170 °C under an argon atmosphere. After 3 h, the reaction mixture was cooled to 110 °C, water was added and the mixture was stirred overnight at room temperature. The precipitate that formed was collected by filtration, washed with water (4 × 20 mL) and purified by flash chromatography to provide the desired compounds **18** and **19**. Compound **26** was prepared similarly from 2-thiohydantoin (1.1 equiv) and benzaldehyde **3b**.

General procedure 4: Synthesis of 5-benzylimidazoline-2,4-dione (hydantoin) fragments.

To a solution of **18** or **19** (1 equiv) in absolute EtOH was added Pd/C (40% by weight of **18** or **19**). The reaction mixture was stirred at room temperature overnight under an atmosphere of hydrogen. After completion of reaction (as evidenced by TLC), the reaction mixture was

filtered through celite and the celite washed with MeOH (15-20 mL). The solvent was evaporated in vacuo and the crude residue purified by flash chromatography to provide the fragments **20** and **21**.

General procedure 5: Synthesis of 5-benzylidenethiazolidine-2,4-dione or 5-benzylidene-2-sulfanylidene-1,3-thiazolidin-4-one (thiazolidinedione and rhodanine) fragments.

To an appropriate benzaldehyde **3a** or **3b** (1 equiv) in dry toulene (10-15 mL) at room temperature, was added rhodanine (1 equiv) or 2,4-thiazolidinedione (1 equiv) and anhydrous ammonium acetate (1.5 equiv) under argon atmosphere. The resultant reaction mixture stirred at 90-100 °C for 3 h. After 3 h, the precipitate of the desired product was filtered and washed with Et_2O (2 × 15 mL). The crude solid was recrystallised in absolute EtOH to provide the desired compounds as described in the series of **16** and **22-23**.

General procedure 6: Synthesis of 5-benzyl-2-sulfanylidene-1,3-thiazolidin-4-one or 5-Benzylthiazolidine-2,4-dione (thiazolidinedione and rhodanine) fragments.

To a stirred solution of appropriate compound **16** or **22** or **23** (1 equiv) in dry pyridine (0.81 mL/mmol) and dry THF (0.66 mL/mmol), was added 2.0 M $LiBH_4$ in THF (2.2 equiv) at room temperature and under argon atmosphere (Effervescences were controlled by addition rate of $LiBH_4$ solution). The resulting mixture was refluxed for 3-4 h. After completion of reaction (as evidenced by TLC), the reaction mixture was quenched by 1N HCl (1-2 mL), extracted with EtOAc (3 × 15 mL). The combined organic layers were washed with brine (1 × 10 mL), dried over $MgSO_4$ and concentrated in vacuo. The crude residue was purified by flash chromatography to provide the desired compounds as described in the series of **17** and **24-25**.

Ethyl 2-hydroxy-2-phenylacetate (2a)[66]

Compound **2a** was synthesized from ethyl glyoxylate 50% solution in toulene (0.59 mL, 3.0 mmol) and compound **1a** (0.548 g, 4.50 mmol) according to general procedure 1. The crude residue was purified by flash chromatography (Gradient: 8−10 % EtOAc in *n*-hexane) to afford the title compound as a colorless oil (0.394 g, 72.96%). R_f = 0.46 (30% EtOAc in *n*-hexane). ^{1}H NMR (500 MHz, $CDCl_3$) δ_H = 7.43-7.41 (m, 2H, H_{Ar}), 7.38-7.35 (m, 2H, H_{Ar}), 7.34-7.31 (m, 1H, H_{Ar}), 5.16 (d, J = 5.25 Hz, 1H, OH-C<u>H</u>), 4.30-4.24 (m, 1H, C<u>H</u>H-CH_3), 4.21-4.14 (m, 1H, CH<u>H</u>-CH_3), 3.47 (d, J = 5.7 Hz, 1H, CH-O<u>H</u>), 1.23 (t, J = 7.15 Hz, 3H, CH_2-C<u>H</u>$_3$), general assignments were confirmed by ^{1}H-^{1}H gCOSY. ^{13}C NMR (125 MHz, $CDCl_3$) δ_C = 173.8 (C=O), 138.6 (C_{quat}), 128.7 (2 × CH_{Ar}), 128.5 (CH_{Ar}), 126.7 (2 × CH_{Ar}), 73.0 (OH-CH), 62.4 (<u>C</u>H_2-CH_3), 14.2 (CH_2-<u>C</u>H_3), general assignments were confirmed by ^{1}H-^{13}C HSQC. LRMS-ESI: *m/z* = 203 $[M + Na]^+$.

Ethyl 2-(2,4-dimethoxyphenyl)-2-hydroxyacetate (2b)[66, 72]

The compound **2b** was synthesized from ethyl glyoxylate 50% solution in toulene (0.19 mL, 1.0 mmol) and compound **1a** (0.272 g, 1.5 mmol) according to general procedure 1. The crude residue was purified by flash chromatography (Gradient: 8−10% EtOAc in *n*-hexane) to afford the title compound as a pale yellow oil (0.209 g, 87.08%). R_f = 0.39 (30% EtOAc in *n*-hexane). ^{1}H NMR (500 MHz, DMSO-d_6) δ_H = 7.20 (d, J = 8.4 Hz, 1H, H_{Ar}), 6.54 (d, J_{meta} = 2.4 Hz, 1H, H_{Ar}), 6.51 (dd, $J_{ortho,\ meta}$ = 8.35, 2.4 Hz, 1H, H_{Ar}), 5.66 (d, J = 6.05 Hz, 1H, OH-C<u>H</u>), 5.20 (d, J = 6.05 Hz, 1H, CH-O<u>H</u>), 4.09-4.02 (m, 2H, C<u>H</u>$_2$-CH_3), 3.75 (s, 6H, 2 × OCH_3), 1.12 (t, J = 7.1 Hz, 3H, CH_2-C<u>H</u>$_3$), general assignments were confirmed by ^{1}H-^{1}H gCOSY. ^{13}C NMR (125 MHz, DMSO-d_6) δ_C = 172.9 (C=O), 160.3 (C_{quat}), 157.4 (C_{quat}), 128.7 (CH_{Ar}), 120.6 (C_{quat}), 104.7 (CH_{Ar}), 98.3 (CH_{Ar}), 66.9 (OH-CH), 60.0 (<u>C</u>H_2-CH_3), 55.5

(OCH_3), 55.2 (OCH_3), 14.1 (CH_2-$\underline{C}H_3$), general assignments were confirmed by ^{1}H-^{13}C HSQC. LRMS-ESI: *m/z* = 263 $[M + Na]^+$.

5-Phenyl-1,3-oxazolidine-2,4-dione (10)

The compound **10** was synthesized from compound **2a** (0.179 g, 0.99 mmol) according to general procedure 2. The crude residue was purified by flash chromatography (Gradient: 15−20% EtOAc in *n*-hexane) to afford the title compound as a white solid (0.030 g, 17.04%). R_f = 0.34 (30% EtOAc in *n*-hexane). Mp = 100−102°C. ^{1}H NMR (500 MHz, DMSO-d_6) δ_H = 12.15 (s, 1H, NH), 7.46-7.44 (m, 3H, H_{Ar}), 7.41-7.40 (m, 2H, H_{Ar}), 6.04 (s, 1H, O-CH-CO), general assignments were confirmed by ^{1}H-^{1}H gCOSY. ^{13}C NMR (125 MHz, DMSO-d_6) δ_C = 173.5 (C=O), 155.6 (C=O), 132.8 (C_{quat}), 129.5 (CH_{Ar}), 128.9 (2 × CH_{Ar}), 126.8 (2 × CH_{Ar}), 81.0 (O-$\underline{C}$H-CO), general assignments were confirmed by ^{1}H-^{13}C HSQC. LRMS-ESI: *m/z* = 176 $[M - H]^+$. HRMS-ESI: $[M - H]^+$ calcd for $C_9H_6NO_3$, 176.0342, found 176.0352.

5-(2,4-Dimethoxyphenyl)-1,3-oxazolidine-2,4-dione (11)

The compound **11** was synthesized from compound **2b** (0.19 g, 0.79 mmol) according to general procedure 2. The crude residue was purified by flash chromatography (Gradient: 4−5% MeOH in DCM) to afford the title compound as a white solid (0.035 g, 18.71%). R_f = 0.58 (10% MeOH in DCM). Mp = 180−182°C. ^{1}H NMR (500 MHz, DMSO-d_6) δ_H = 11.86 (s, 1H, NH), 7.29 (d, J_{ortho} = 8.4 Hz, 1H, H_{Ar}), 6.63 (d, J_{meta} = 2.35 Hz, 1H, H_{Ar}), 6.56 (dd, $J_{ortho,\ meta}$ = 8.4, 2.4 Hz, 1H, H_{Ar}), 5.89 (s, 1H, O-CH-CO), 3.79 (s, 3H, OCH_3), 3.74 (s, 3H, OCH_3), general assignments were confirmed by ^{1}H-^{1}H gCOSY. ^{13}C NMR (125 MHz, DMSO-d_6) δ_C = 174.3 (C=O), 162.4 (C=O), 159.3 (C_{quat}), 155.9 (C_{quat}), 132.9 (CH_{Ar}), 112.8 (C_{quat}), 105.1 (CH_{Ar}), 99.1 (CH_{Ar}), 79.8 (O-$\underline{C}$H-CO), 55.9 (OCH_3), 55.5 (OCH_3), general

assignments were confirmed by ^{1}H-^{13}C HSQC. LRMS-ESI: *m/z* = 236 [M − H]$^{+}$. HRMS-ESI: [M + Na]$^{+}$ calcd for $C_{11}H_{11}NNaO_5$, 260.0529, found 260.0529.

5-Phenyl-1,3-thiazolidine-2,4-dione (13)

The compound **13** was synthesized from compound **2a** (0.45 g, 2.5 mmol) according to general procedure 2. The crude residue was purified by flash chromatography (gradient: 10−15% EtOAc in *n*-hexane) to afford the title compound as a white solid (0.020 g, 4.14%). R_f = 0.37 (30% EtOAc in *n*-hexane). Mp = 134−136°C. ^{1}H NMR (500 MHz, DMSO-d_6) δ_H = 13.55 (s, 1H, NH), 7.49-7.47 (m, 3H, H_{Ar}), 7.38-7.36 (m, 2H, H_{Ar}), 6.27 (s, 1H, S-CH-CO), general assignments were confirmed by ^{1}H-^{1}H gCOSY. ^{13}C NMR (125 MHz, DMSO-d_6) δ_C = 192.1 (C=O), 174.7 (C=O), 132.5 (C_{quat}), 130.3 (CH_{Ar}), 129.7 (2 × CH_{Ar}), 127.5 (2 × CH_{Ar}), 84.8 (S-<u>C</u>H-CO), general assignments were confirmed by ^{1}H-^{13}C HSQC. LRMS-ESI: *m/z* = 192 [M − H]$^{+}$. HRMS-ESI: [M − H]$^{+}$ calcd for $C_9H_6NO_2S$, 192.0114, found 192.0127.

5-(2,4-Dimethoxyphenyl)-2-thioxo-1,3-oxazolidin-4-one (14)

The compound **14** was synthesized from compound **2b** (0.385 g, 1.60 mmol) according to general procedure 2. The crude residue was purified by flash chromatography (gradient: 10−20% EtOAc in *n*-hexane) to afford the title compound as a colorless oil (0.013 g, 3.20%). ^{1}H NMR (500 MHz, DMSO-d_6) δ_H = 13.25 (s, 1H, NH), 7.31 (d, *J* = 8.45 Hz, 1H, H_{Ar}), 6.65 (d, *J* = 2.35 Hz, 1H, H_{Ar}), 6.59 (dd, *J* = 8.35, 2.4 Hz, 1H, H_{Ar}), 6.10 (s, 1H, O-CH-CO), 3.80 (s, 3H, OCH_3), 3.74 (s, 3H, OCH_3). ^{13}C NMR (125 MHz, DMSO-d_6) δ_C = 173.03 (C=O), 160.4 (C=S), 157.5 (C_{quat}), 128.8 (CH_{Ar}), 120.6 (CH_{Ar}), 112.2 (C_{quat}), 104.8 (CH_{Ar}), 98.4 (C_{quat}), 83.1 (O-<u>C</u>H-CO), 55.6 (OCH_3), 55.3 (OCH_3). LRMS-ESI: *m/z* = 252 [M − H]$^{+}$.

5-[(2,4-Dimethoxyphenyl)methylidene]-1,3-thiazolidine-2,4-dione (16)

The compound **16** was synthesized from compound **3b** (0.50 g, 3.01 mmol) according to general procedure 5. The crude residue was recrystallised from EtOH to afford the title compound as a yellow solid (0.56 g, 70.26%). R_f = 0.60 (30% EtOAc in *n*-hexane). Mp = 240−242°C, decomposition. ^{1}H NMR (500 MHz, DMSO-d_6) δ_H = 12.43 (s, 1H, NH), 7.92 (s, 1H, Ph-CH=C), 7.33 (d, J_{ortho} = 8.6 Hz, 1H, H_{Ar}), 6.70 (dd, $J_{ortho,\ meta}$ = 8.65, 2.35 Hz, 1H, H_{Ar}), 6.67 (d, J_{meta} = 2.25 Hz, 1H, H_{Ar}), 3.89 (s, 3H, OCH_3), 3.84 (s, 3H, OCH_3), general assignments were confirmed by ^{1}H-^{1}H gCOSY. ^{13}C NMR (125 MHz, DMSO-d_6) δ_C = 168.2 (C=O), 167.6 (C=O), 163.1 (C_{quat}), 159.8 (C_{quat}), 130.1 (CH_{Ar}), 126.5 (Ph-<u>C</u>H=C), 119.9 (C_{quat}), 114.3 (C_{quat}), 106.5 (CH_{Ar}), 98.6 (CH_{Ar}), 55.9 (OCH_3), 55.6 (OCH_3), general assignments were confirmed by ^{1}H-^{13}C HSQC. LRMS-ESI: *m/z* = 266 $[M + H]^+$, 288 $[M + Na]^+$. HRMS-ESI: $[M + H]^+$ calcd for $C_{12}H_{12}NO_4S$, 266.0482, found 266.0481.

5-[(2,4-Dimethoxyphenyl)methyl]-1,3-thiazolidine-2,4-dione (17)

The compound **17** was synthesized from compound **16** (0.15 g, 0.57 mmol) according to general procedure 6. The crude residue was purified by flash chromatography (Gradient: 15−20% EtOAc in *n*-hexane) to afford the title compound as (0.060 g, 39.73%). R_f = 0.33 (30% EtOAc in *n*-hexane). Mp = 169−171°C. ^{1}H NMR (500 MHz, DMSO-d_6) δ_H = 12.01 (s, 1H, NH), 7.04 (d, J_{ortho} = 8.3 Hz, 1H, H_{Ar}), 6.54 (d, J_{meta} = 2.4 Hz, 1H, H_{Ar}), 6.46 (dd, $J_{ortho,\ meta}$ = 8.3, 2.4 Hz, 1H, H_{Ar}), 4.78 (dd, J = 10.0, 4.55 Hz, 1H, Ph-CH_2-C<u>H</u>), 3.78 (s, 3H, OCH_3), 3.74 (s, 3H, OCH_3), 3.40 (dd, J = 13.9, 4.5 Hz, 1H, Ph-C<u>H</u>H-CH), 2.87 (dd, J = 13.9, 10.0 Hz, 1H, Ph-CH<u>H</u>-CH), general assignments were confirmed by ^{1}H-^{1}H gCOSY. ^{13}C NMR (125 MHz, DMSO-d_6) δ_C = 175.9 (C=O), 171.8 (C=O), 159.9 (C_{quat}), 158.2 (C_{quat}), 130.8 (CH_{Ar}), 117.1 (C_{quat}), 104.5 (CH_{Ar}), 98.4 (CH_{Ar}), 55.4 (OCH_3), 55.1 (OCH_3), 51.8 (Ph-CH_2-<u>C</u>H), 32.2 (Ph-<u>C</u>H_2-CH), general assignments were confirmed by ^{1}H-^{13}C HSQC. LRMS-

ESI: *m/z* = 268[M + H]$^+$, 290 [M + Na]$^+$. HRMS-ESI: [M + Na]$^+$ calcd for $C_{12}H_{13}NNaO_4S$, 290.0458, found 290.0458.

5-(Phenylmethylidene)imidazolidine-2,4-dione (18)

The compound **18** was synthesized from compound **3a** (1.00 g, 9.42 mmol) according to general procedure 3. The crude residue was purified by flash chromatography (Gradient: 20−25% EtOAc in *n*-hexane) to afford the title compound as a yellow solid (1.30 g, 73.44 %). R_f = 0.17 (30% EtOAc in *n*-hexane). Mp = 270−275°C, decomposition. ^{1}H NMR (500 MHz, DMSO-d_6) δ_H = 7.61 (d, J_{ortho} = 7.25 Hz, 2H, H_{Ar}), 7.37 (t, J_{ortho} = 7.85 Hz, 2H, H_{Ar}), 7.30-7.27 (m, 1H, H_{Ar}), 6.30 (s, 1H, Ph-CH=C), NH protons are in exchange, general assignments were confirmed by ^{1}H-^{1}H gCOSY. ^{13}C NMR (125 MHz, DMSO-d_6) δ_C = 165.9 (C=O), 156.0 (C=O), 133.1 (C_{quat}), 129.5 (2 × CH_{Ar}), 129.0 (2 × CH_{Ar}), 128.6 (CH_{Ar}), 128.2 (C_{quat}), 108.5 (Ph-<u>C</u>H=C), general assignments were confirmed by ^{1}H-^{13}C HSQC. LRMS-ESI: *m/z* = 189 [M + H]$^+$. HRMS-ESI: [M + Na]$^+$ calcd for $C_{10}H_8N_2NaO_2$, 211.0478, found 211.0477.

5-[(2,4-Dimethoxyphenyl)methylidene]imidazolidine-2,4-dione (19)

The compound **19** was synthesized from compound **3b** (1.00 g, 6.02 mmol) according to general procedure 3. The crude residue was purified by flash chromatography (Gradient: 60−80% EtOAc in *n*-hexane) to afford the title compound as a yellow solid (0.850 g, 56.97%). R_f = 0.55 (50% EtOAc in *n*-hexane). Mp = 230−232°C. ^{1}H NMR (500 MHz, DMSO-d_6) δ_H = 7.56 (d, J_{ortho} = 8.45 Hz, 1H, H_{Ar}), 6.61-6.60 (m, 2H, H_{Ar} and Ph-CH-C), 6.55 (d, J_{ortho} = 8.30 Hz, 1H, H_{Ar}), 3.84 (s, 3H, OCH_3), 3.81 (s, 3H, OCH_3), NH protons are in exchange, general assignments were confirmed by ^{1}H-^{1}H gCOSY. ^{13}C NMR (125 MHz, DMSO-d_6) δ_C = 166.1 (C=O), 161.6 (C=O), 159.1 (C_{quat}), 156.0 (C_{quat}), 130.6 (CH_{Ar}), 126.5

(C_{quat}), 114.7 (C_{quat}), 106.0 (CH_{Ar}), 103.5 (CH_{Ar}), 98.7 (Ph-CH=C), 56.2 (OCH_3), 55.9 (OCH_3), general assignments were confirmed by ^{1}H-^{13}C HSQC. LRMS-ESI: *m/z* = 249 [M + H]$^+$. HRMS-ESI: [M + H]$^+$ calcd for $C_{12}H_{13}N_2O_4$, 249.0870, found 249.0869.

5-Benzylimidazolidine-2,4-dione (20)

The compound **20** was synthesized from compound **18** (0.10 g, 0.53 mmol) according to general procedure 4. The crude residue was purified by flash chromatography (Gradient: 50−60% EtOAc in *n*-hexane) to afford the title compound as a white solid (0.09 g, 89.10%). R_f = 0.17 (50% EtOAc in *n*-hexane). Mp = 191−193°C. ^{1}H NMR (500 MHz, DMSO-d_6) δ_H = 10.43 (s, 1H, NH), 7.91 (s, 1H, NH), 7.29-7.26 (m, 2H, H_{Ar}), 7.23-7.21 (m, 1H, H_{Ar}), 7.19-7.18 (m, 2H, H_{Ar}), 4.32 (t, *J* = 5.85 Hz, 1H, Ph-CH_2-CH), 2.97-2.93 (m, 1H, Ph-CHH-CH), 2.93-2.89 (m, 1H, Ph-CHH-CH), general assignments were confirmed by ^{1}H-^{1}H gCOSY. ^{13}C NMR (125 MHz, DMSO-d_6) δ_C = 175.2 (C=O), 156.2 (C=O), 135.6 (C_{quat}), 129.7 (2 × CH_{Ar}), 128.1 (2 × CH_{Ar}), 126.6 (CH_{Ar}), 58.4 (Ph-CH_2-CH), 36.4 (Ph-CH_2-CH), general assignments were confirmed by ^{1}H-^{13}C HSQC. LRMS-ESI: *m/z* = 191 [M + H]$^+$, 213 [M + Na]$^+$. HRMS-ESI: [M + Na]$^+$ calcd for $C_{10}H_{10}N_2NaO_2$, 213.0635, found 213.0634.

5-[(2,4-Dimethoxyphenyl)methyl]imidazolidine-2,4-dione (21)

The compound **21** was synthesized from compound **19** (0.10 g, 0.40 mmol) according to general procedure 4. The crude residue was purified by flash chromatography (Gradient: 30−40% EtOAc in *n*-hexane) to afford the title compound as a white solid (0.055 g, 55.0%). R_f = 0.13 (50% EtOAc in *n*-hexane). Mp = 165−167°C. ^{1}H NMR (500 MHz, DMSO-d_6) δ_H = 10.49 (s, 1H, NH), 7.69 (s, 1H, NH), 7.02 (d, J_{ortho} = 8.25 Hz, 1H, H_{Ar}), 6.52 (d, J_{meta} = 2.4 Hz, 1H, H_{Ar}), 6.44 (dd, $J_{ortho,\ meta}$ = 8.3, 2.4 Hz, 1H, H_{Ar}), 4.19-4.16 (m, 1H, Ph-CH_2-CH), 3.75 (s, 3H, OCH_3), 3.74 (s, 3H, OCH_3), 2.98 (dd, *J* = 13.9, 4.95 Hz, 1H, Ph-CHH-CH), 2.65

(dd, J = 13.9, 7.45 Hz, 1H, Ph-CH<u>H</u>-CH), general assignments were confirmed by ^{1}H-^{1}H gCOSY. ^{13}C NMR (125 MHz, DMSO-d_6) δ_C = 175.5 (C=O), 159.6 (C=O), 158.3 (C_{quat}), 157.3 (C_{quat}), 131.3 (CH_{Ar}), 116.4 (C_{quat}), 104.4 (CH_{Ar}), 98.2 (CH_{Ar}), 57.6 (Ph-CH_2-<u>C</u>H), 55.4 (OCH_3), 55.1 (OCH_3), 31.6 (Ph-<u>C</u>H_2-CH), general assignments were confirmed by ^{1}H-^{13}C HSQC. LRMS-ESI: m/z = 251 $[M + H]^+$, 273 $[M + Na]^+$. HRMS-ESI: $[M + Na]^+$ calcd for $C_{12}H_{14}N_2NaO_4$, 273.0846, found 273.0845.

5-(Phenylmethylidene)-2-sulfanylidene-1,3-thiazolidin-4-one (22)

The compound **22** was synthesized from compound **3a** (0.50 g, 4.71 mmol) according to general procedure 5. The crude residue was recrystallised from EtOH to afford the title compound as a yellow solid (0.6 g, 57.63%). R_f = 0.54 (30% EtOAc in *n*-hexane). Mp = 204−206°C. ^{1}H NMR (500 MHz, DMSO-d_6) δ_H = 13.84 (s, 1H, NH), 7.64 (s, 1H, Ph-CH=C), 7.60-7.59 (m, 2H, H_{Ar}), 7.55-7.48 (m, 3H, H_{Ar}), general assignments were confirmed by ^{1}H-^{1}H gCOSY. ^{13}C NMR (125 MHz, DMSO-d_6) δ_C = 195.7 (C=S), 169.4 (C=O), 133.0 (C_{quat}), 131.6 (Ph-<u>C</u>H=C), 130.7 (CH_{Ar}), 130.5 (2 × CH_{Ar}), 129.4 (2 × CH_{Ar}), 125.5 (C_{quat}), general assignments were confirmed by ^{1}H-^{13}C HSQC. LRMS-ESI: m/z = 220 $[M - H]^+$. HRMS-ESI: $[M - H]^+$ calcd for $C_{10}H_6NOS_2$, 219.9885, found 219.9897.

5-[(2,4-Dimethoxyphenyl)methylidene]-2-sulfanylidene-1,3-thiazolidin-4-one (23)

The compound **23** was synthesized from compound **3b** (0.50 g, 3.01 mmol) according to general procedure 5. The crude residue was recrystallised from EtOH to afford the title compound as a yellow solid (0.7 g, 82.84%). R_f = 0.31 (30% EtOAc in *n*-hexane). Mp = 273−275°C, decomposition. ^{1}H NMR (500 MHz, DMSO-d_6) δ_H = 13.65 (s, 1H, NH), 7.74 (s, 1H, Ph-CH=C), 7.33 (d, J_{ortho} = 8.65 Hz, 1H, H_{Ar}), 6.71 (dd, $J_{ortho,\ meta}$ = 8.65, 2.3Hz, 1H, H_{Ar}), 6.68 (s, 1H, H_{Ar}), 3.90 (s, 3H, OCH_3), 3.85 (s, 3H, OCH_3), general assignments were

confirmed by ^{1}H-^{1}H gCOSY. ^{13}C NMR (125 MHz, DMSO-d_6) δ_C = 195.8 (C=S), 169.5 (C=O), 163.6 (C_{quat}), 160.0 (C_{quat}), 131.4 (CH_{Ar}), 127.0 (Ph-<u>C</u>H=C), 121.7 (C_{quat}), 114.3 (C_{quat}), 106.9 (CH_{Ar}), 98.6 (CH_{Ar}), 55.9 (OCH_3), 55.7 (OCH_3), general assignments were confirmed by ^{1}H-^{13}C HSQC. LRMS-ESI: *m/z* = 280 $[M - H]^+$. HRMS-ESI: $[M - H]^+$ calcd for $C_{12}H_{10}NO_3S_2$, 280.0097, found 280.0107.

5-Benzyl-2-sulfanylidene-1,3-thiazolidin-4-one (24)

The compound **24** was synthesized from compound **22** (0.10 g, 0.45 mmol) according to general procedure 6. The crude residue was purified by flash chromatography (Gradient: 15−20% EtOAc in *n*-hexane) to afford the title compound as a white solid (0.021 g, 21.0 %). R_f = 0.34 (30% EtOAc in *n*-hexane). Mp = 119−121°C. ^{1}H NMR (500 MHz, DMSO-d_6) δ_H = 13.16 (s, 1H, NH), 7.33-7.23 (m, 5H, H_{Ar}), 5.04 (dd, *J* = 8.9, 4.6 Hz, 1H, Ph-CH_2-C<u>H</u>), 3.37 (dd, *J* = 14.1, 4.45 Hz, 1H, Ph-C<u>H</u>H-CH), 3.17 (dd, *J* = 14.1, 9.1 Hz, 1H, Ph-CH<u>H</u>-CH), general assignments were confirmed by ^{1}H-^{1}H gCOSY. ^{13}C NMR (125 MHz, DMSO-d_6) δ_C = 203.3 (C=S), 177.9 (C=O), 136.6 (C_{quat}), 129.2 (2 × CH_{Ar}), 128.5 (2 × CH_{Ar}), 127.1 (CH_{Ar}), 55.7 (Ph-CH_2-<u>C</u>H), 36.5 (Ph-<u>C</u>H_2-CH), general assignments were confirmed by ^{1}H-^{13}C HSQC. LRMS-ESI: *m/z* = 222 $[M - H]^+$. HRMS-ESI: $[M - H]^+$ calcd for $C_{10}H_8NOS_2$, 222.0042, found 222.0054.

5-[(2,4-Dimethoxyphenyl)methyl]-2-sulfanylidene-1,3-thiazolidin-4-one (25)

The compound **25** was synthesized from compound **23** (0.20 g, 0.71 mmol) according to general procedure 6. The crude residue was purified by flash chromatography (Gradient: 12−15% EtOAc in *n*-hexane) to afford the title compound as a yellow solid (0.095 g, 47.26%). R_f = 0.53 (30% EtOAc in *n*-hexane). Mp = 160−162°C. ^{1}H NMR (500 MHz, DMSO-d_6) δ_H = 13.15 (s, 1H, NH), 7.04 (d, J_{ortho} = 8.25 Hz, 1H, H_{Ar}), 6.54 (d, J_{meta} = 2.4 Hz,

1H, H_{Ar}), 6.46 (dd, $J_{ortho, meta}$ = 8.3, 2.4 Hz, 1H, H_{Ar}), 4.90 (dd, J = 9.6, 4.85 Hz, 1H, Ph-CH_2-C<u>H</u>), 3.77 (s, 3H, OCH_3), 3.74 (s, 3H, OCH_3), 3.36 (dd, J = 13.95, 4.85 Hz, 1H, Ph-C<u>H</u>H-CH), 2.95 (dd, J = 14.0, 9.6 Hz, 1H, Ph-CH<u>H</u>-CH), general assignments were confirmed by ^{1}H-^{1}H gCOSY. ^{13}C NMR (125 MHz, DMSO-d_6) δ_C = 203.6 (C=S), 178.2 (C=O), 160.0 (C_{quat}), 158.1 (C_{quat}), 130.8 (CH_{Ar}), 116.9 (C_{quat}), 104.6 (CH_{Ar}), 98.4 (CH_{Ar}), 55.4 (OCH_3), 55.2 (OCH_3), 54.8 (Ph-CH_2-<u>C</u>H), 31.6 (Ph-<u>C</u>H_2-CH), general assignments were confirmed by ^{1}H-^{13}C HSQC. LRMS-ESI: m/z = 282 $[M - H]^+$. HRMS-ESI: $[M - H]^+$ calcd for $C_{12}H_{12}NO_3S_2$, 282.0253, found 282.0263.

5-[(2,4-Dimethoxyphenyl)methylidene]-2-sulfanylideneimidazolidin-4-one (26)

The compound **26** was synthesized from compound **3b** (1.00 g, 6.02 mmol) according to general procedure 3. The crude residue was purified by flash chromatography (Gradient: 10−20% EtOAc in *n*-hexane) to afford the title compound as a yellow solid (0.852 g, 53.52%). R_f = 0.25 (30% EtOAc in *n*-hexane). Mp = 235−237°C. ^{1}H NMR (500 MHz, DMSO-d_6) δ_H = 12.23 (s, 1H, NH), 11.93 (s, 1H, NH), 7.74 (d, J_{ortho} = 8.65 Hz, 1H, H_{Ar}), 6.69 (s, 1H, Ph-CH=C), 6.61 (d, J_{meta} = 2.35 Hz, 1H, H_{Ar}), 6.58 (dd, $J_{ortho, meta}$ = 8.6, 2.4 Hz, 1H, H_{Ar}), 3.86 (s, 3H, OCH_3), 3.83 (s, 3H, OCH_3), general assignments were confirmed by ^{1}H-^{1}H gCOSY. ^{13}C NMR (125 MHz, DMSO-d_6) δ_C = 178.1 (C=S), 165.8 (C=O), 162.1 (C_{quat}), 159.2 (C_{quat}), 131.3 (CH_{Ar}), 125.8 (C_{quat}), 113.7 (C_{quat}), 106.5 (Ph-<u>C</u>H=C), 105.9 (CH_{Ar}), 98.2 (CH_{Ar}), 55.9 (OCH_3), 55.5 (OCH_3), general assignments were confirmed by ^{1}H-^{13}C HSQC. LRMS-ESI: m/z = 265 $[M + H]^+$, 287 $[M + Na]^+$. HRMS (ESI): $[M + H]^+$ calcd for $C_{12}H_{13}N_2O_3S$, 265.0641, found 265.0641.

5-[(2,4-Dimethoxyphenyl)methyl]-2-sulfanylideneimidazolidin-4-one (27)

To 5-benzylidene-2-sulfanylideneimidazolidin-4-one **26** (0.10 g, 0.38 mmol) in glacial acetic acid (2 mL) was added Zn dust (0.272 g, 4.1657 mmol) at room temperature. The resultant

reaction mixture was refluxed for 12-18 h. After completion of reaction (TLC), the reaction mixture was cooled down to 50 °C, added MeOH (5 × acetic acid qty.) refluxed for 5-10 min. The reaction mixture was then filtered through celite bed, washed with MeOH (15-20 mL) and evaporated in vacuo. The crude residue was purified by flash chromatography (Gradient: 15−30% EtOAc in *n*-hexane) to afford the title compound as a yellow solid (0.065 g, 65.0%). R_f = 0.58 (50% EtOAc in *n*-hexane). Mp = 153−155°C. ^{1}H NMR (500 MHz, DMSO-d_6) δ_H = 11.50 (s, 1H, NH), 9.86 (s, 1H, NH), 7.01 (d, J_{ortho} = 8.3 Hz, 1H, H_{Ar}), 6.51 (d, J_{meta} = 2.4 Hz, 1H, H_{Ar}), 6.43 (dd, $J_{ortho,\ meta}$ = 8.3, 2.45 Hz, 1H, H_{Ar}), 4.40-4.38 (m, 1H, Ph-CH_2-C<u>H</u>), 3.76 (s, 3H, OCH_3), 3.74 (s, 3H, OCH_3), 2.96 (dd, J = 14.05, 5.65 Hz, 1H, Ph-C<u>H</u>H-CH), 2.78 (dd, J = 14.05, 6.65 Hz, 1H, Ph-CH<u>H</u>-CH), general assignments were confirmed by ^{1}H-^{1}H gCOSY. ^{13}C NMR (125 MHz, DMSO-d_6) δ_C = 182.3 (C=S), 176.0 (C=O), 159.8 (C_{quat}), 158.4 (C_{quat}), 131.5 (CH_{Ar}), 115.7 (C_{quat}), 104.5 (CH_{Ar}), 98.3 (CH_{Ar}), 60.7 (Ph-CH_2-<u>C</u>H), 55.5 (OCH_3), 55.2 (OCH_3), 30.8 (Ph-<u>C</u>H_2-CH), general assignments were confirmed by ^{1}H-^{13}C HSQC. LRMS-ESI: m/z = 267 $[M + H]^+$, 289 $[M + Na]^+$. HRMS-ESI: $[M + H]^+$ calcd for $C_{12}H_{15}N_2O_3S$, 267.0798, found 267.0798. Compound **27′** was subsequently identified as a ~5% impurity in **27**.

Mass Spectrometry

Prior to mass spectrometric analysis hCA II protein was concentrated and buffer exchanged into 10 mM NH_4OAc pH 7.0 using Amicon Ultra 0.5 centrifugal filters (Merck Millipore, Sydney, NSW, Australia). In detail, 500 µL of the initial protein solution was loaded on the filter and centrifuged at 14,000 × g for 15 min at 4 °C on a Heraeus Pico 21 benchtop centrifuge (Thermo Fisher Scientific Australia Pty Ltd). The flow through was discarded and the concentrate resuspended in 450 µL of 10 mM NH_4OAc pH 7.0. This process was repeated

four times in order to minimise residual salt in the protein sample that may interfere with protein ionisation. The final concentrate was recovered by spinning at 3,000 × g for 1 min according to the manufacturers protocol. Concentration of the proteins was verified for CA II using the absorption at 280 nm combined with an extinction coefficient of 50.42 x 10^3 M^{-1} cm^{-1} and adjusted to a final concentration of 15 μM with 10 mM NH_4OAc, pH 7.0. All test fragments were prepared and stored as 5 mM stock solutions in DMSO.

For experiments with equimolar concentration of protein and fragment, immediately before the mass spectrometric analysis, fragments were diluted in 10 mM NH_4OAc 7.0 pH to a final concentration of 15 μM (0.3% DMSO). hCA II (2.5 μL of 15 μM stock) was mixed with fragment solution (2.5 μL of 15 μM stock). For nanoESI-MS titration experiments, 0.5 μL of the required fragment concentration in DMSO were prepared in assay-ready 96-well microplates by Compounds Australia (www.compoundsaustralia.com). Prior to analysis 14.5 μL of protein (15 μM, 10 mM NH_4OAc) was added to each fragment containing microplate well (final sample 3.3% DMSO). The protein:fragment sample solutions were mixed, then incubated for 10 min at room temperature before nanoESI-MS analysis. The incubation time was selected following time series test experiments which showed that no change in binding is observed after 10 min. FTICR-MS calibration using perfluorohexanoic acid (PFHA) was performed daily while quality control runs of pure CA II were performed before every batch of screening. For nanoESI-MS analysis samples were infused into a Bruker solariX XR™ 12.0 Tesla Fourier Transform Ion Cyclotron Resonance (FT-ICR) mass spectrometer (FT-ICR MS) fitted with a ParaCell™ (Bruker Daltonics Inc., Billerica, MA) using a Triversa Nanomate (Advion BioSciences, Ithaca, NY, USA) automated nanoESI interface fitted with a 5 micron HD A ESI Chip (Advion BioSciences, Ithaca, NY, USA). Spray conditions were

optimized for signal intensity, signal to noise ratio and spray duration. Positive ion ESI was used with a capillary voltage of 1.2 kV and a nitrogen nebulizing gas pressure of 0.4 psi. The FT-ICR mass spectrometer parameters were optimised to maximise signal intensity whilst ensuring gentle enough conditions in order to retain the proteins in a native-like state and avoid in-source dissociation. In detail, data were acquired for at least 45 scans, over the range of *m/z* 500-10,000 with the quadrupole set at *m/z* 600 while a Skimmer 1 voltage of 30 V, a Drying Gas Temperature of 100 ^{o}C, a Nebulizer Gas Flow Rate of 2 bar, a Capillary Voltage of 3,500 V, a Spray Shield of 500 V, a Collision Voltage (Entrance) of -3.0 V, a DC Extract Bias of 0.1 V, a Collision Cell RF of 2,000 Vpp, an Ion Accumulation Time of 0.001 sec and a Flight Time of 2.1 msec were used. Mass spectra were processed with Bruker Compass DataAnalysis 4.2 (Bruker Daltonics Inc., Billerica, MA). For the peak determination and intensity calculation, SNAP algorithm version 2.0 was used with a signal to noise threshold set at 3 and quality factor threshold set at 0.5.

The FB_{MS} for each fragment concentration was assigned as the ratio of the measured intensity of the fragment-bound protein $I_{(P:F)}$ peak to the sum of the unbound protein $I_{(P)}$ and fragment-bound protein $I_{(P:F)}$ peaks for each spectrum, expressed as a percentage (Equation 1). Unbound protein $I_{(P)}$ included both free protein and protein bound to acetate, the latter complex is preserved due to the very gentle electrospray ionisation conditions employed.

$$\mathrm{FB}_{MS} = \frac{\mathrm{I}_{[\mathrm{P:F}]}}{\mathrm{I}_{[\mathrm{P:F}]}+\mathrm{I}_{[P]}} \times 100\% \qquad \text{(Equation 1)}$$

All three observed charge states (+9, +10 and +11) where utilised for the FB_{MS} calculations and compared to FB_{MS} calculations using the predominant charge state (+10). For the analyses of the saturation binding experiments we employed the nonlinear Hill model.[73] The

calculation of K_D value as well as curve fitting were performed by applying the Specific binding with Hill Slope equation in GraphPad Prism 7.01 (Equation 2), also using all three observed charge states (+9, +10 and +11) and the single, predominant charge state (+10) for comparison.

$$\frac{\text{Bound}}{\text{TotalProtein}} = \text{Bmax} * \frac{\text{FragmentConcentration}^{\text{h}}}{\text{Kd}^{\text{h}} + \text{FragmentConcentration}^{\text{h}}} \quad \text{(Equation 2)}$$

In Equation 2 *Bmax* corresponds to the maximum specific binding, *Kd* to the fragment concentration needed to achieve a half-maximum binding at equilibrium and *h* to the Hill slope, which equals 1.0 when a monomer fragment binds to a single site of the protein.

SPR

hCA II protein was expressed and purified as previously described.[22] SPR measurement of fragments interacting with immobilised hCA II were performed using a previously published methodology.[29] All SPR experiments were performed at 25 °C using a Biacore T200 instrument. Minimally biotinylated hCA II protein was immobilised onto a Streptavidin chip surface with instrumental fluidics primed with fragment binding buffer (50 mM HEPES pH 7.4, 0.15 M NaCl, 0.05% Tween-20, 2% [v/v] DMSO). Fresh 100 mM DMSO fragment solutions were diluted directly with the fragment binding buffer to a final concentration of 200 μM and then diluted down 2-fold to 12.5 μM aiming for a 5-point concentration series range for the SPR dose-response experiments. Each compound was injected for 30 s association and 60 s dissociation. Scrubber 2 software package (www.biologic.com.au) was utilised for data processing and analysis.[74] To determine K_D values from dose-response experiments, binding responses at equilibrium were fit to a 1:1 steady state affinity model available within Scrubber.

Protein X-ray Crystallography

Concentrated hCA II at ~10 mg mL^{-1} was set up in SD-2 plates (Molecular Dimensions) with the following ratio of protein plus reservoir plus seeds: 250 nL + 225 nL + 25 nL. The plate was incubated at 8 ºC and the reservoir condition consisted of 2.9 M $(NH_4)_2SO_4$ with 0.1 M Tris buffer at pH 8.3. Dry compound was added to the crystallisation drop after crystals had formed and several days before data were collected. 360 frames of one degree oscillation were taken at the MX-1 beamline of the Australian Synchrotron. The data were indexed using XDS[75] and scaled using Aimless.[76] Molecular replacement was done using Phaser[77] using 4cq0 as the initial starting model. The model was manually rebuilt using Coot[78] and refined using Refmac.[79] The compound was placed in density using the program Afitt (OpenEye Scientific Software) and further refined using Refmac.[79] The structure and structure factors were deposited in the PDB with accession codes: 5TXY, 5TY8, 5TY9, 5TYA, 5U0D, 5U0E, 5U0F, 5U0G and 5VGY.

Crystals with compound **10** (PDB code 5TXY) were also generated by co-crystallisation. For these crystals, a six molar excess of compound to protein was added prior to the protein being set up in crystallisation trials. The data were processed as above, but Phenix[80] was used to refine the structure. eLBOW[81] was used to generate the cif dictionary file and the ligand was manually placed into density.

Corresponding author

S.-A.P. Telephone: +61 7 3735 7825; e-mail: s.poulsen@griffith.edu.au

T.S.P. Telephone: +61 3 9662 7304; e-mail: tom.peat@csiro.au

Acknowledgement

This research was financed by the Australian Research Council (Grant numbers DP140101495, FT10100185). We thank Griffith University for PhD Scholarship to P.M. cDNA for CA II was kindly provided by C. Fierke. We thank OpenEye Scientific Software for a license to use Afitt, the CSIRO Collaborative Crystallisation Centre (www.csiro.au/c3) for crystallisation, and the Australian Synchrotron and the beamline scientists at the MX-1 beamline for their support in data collection. We thank J. Bentley for help with protein purification, M. Hattarki for SPR technical assistance, J. Ryan and T. Nebl for chemistry and mass spectrometry advice. We thank Compounds Australia staff for assistance in the production of assay-ready microplates (www.compoundsaustralia.com).

Abbreviations Used

FBDD, fragment based drug discovery; CA, carbonic anhydrase; CSIRO, Commonwealth Scientific and Industrial Research Organisation; HTS, high throughput screening; K_D, dissociation constant; SPR, surface plasmon resonance; MS, mass spectrometry; FB_{MS}, Fragment Binding by mass spectrometry; FDA, food and drug administration; HEPES, 4-(2-hydroxyethyl)-1-piperazineethanesulfonic acid; PBS, phosphate buffered saline; XRC, X-ray crystallography

Supporting Information. Data collection and structure refinement statistics of fragment:hCA II crystal structures, NMR spectra and SPR sensorgrams for compounds, molecular formula strings for compounds and calculated properties for selected compounds. This material is available free of charge via the Internet at http://pubs.acs.org.

PDB ID Codes. All of the coordinates and structure factors have been deposited in the PDB and are available with the following codes: 5TXY, 5TY8, 5TY9, 5TYA, 5U0D, 5U0E, 5U0F, 5U0G, 5VGY. Authors will release the atomic coordinates and experimental data upon article publication.

References

1. Rouffet, M.; Cohen, S. M. Emerging trends in metalloprotein inhibition. *Dalton Trans.* **2011**, *40*, 3445-3454.

2. Anzellotti, A. I.; Farrell, N. P. Zinc metalloproteins as medicinal targets. *Chem. Soc. Rev.* **2008**, *37*, 1629-1651.

3. Supuran, C. T. Carbonic anhydrase inhibitors in the treatment and prophylaxis of obesity. *Expert Opin. Ther. Patents* **2003**, *13*, 1545-1550.

4. Bull, S.; Loudon, M.; Francis, J. M.; Joseph, J.; Gerry, S.; Karamitsos, T. D.; Prendergast, B. D.; Banning, A. P.; Neubauer, S.; Myerson, S. G. A prospective, double-blind, randomized controlled trial of the angiotensin-converting enzyme inhibitor Ramipril In Aortic Stenosis (RIAS trial). *Eur. Heart J. Cardiovasc Imaging* **2015**, *16*, 834-841.

5. Paris, M.; Porcelloni, M.; Binaschi, M.; Fattori, D. Histone deacetylase inhibitors: from bench to clinic. *J. Med. Chem.* **2008**, *51*, 1505-1529.

6. Fernandez-Montero, J. V.; Vispo, E.; Soriano, V. Emerging antiretroviral drugs. *Expert Opin. Pharmacother.* **2014**, *15*, 211-219.

7. Zastrow, M. L.; Pecoraro, V. L. Designing hydrolytic zinc metalloenzymes. *Biochemistry* **2014**, *53*, 957-978.

8. Andreini, C.; Banci, L.; Bertini, I.; Rosato, A. Counting the zinc-proteins encoded in the human genome. *J. Proteome Res.* **2006**, *5*, 196-201.

9. Martin, D. P.; Blachly, P. G.; McCammon, J. A.; Cohen, S. M. Exploring the influence of the protein environment on metal-binding pharmacophores. *J. Med. Chem.* **2014**, *57*, 7126-7135.

10. Zhang, X. X.; Liao, C. Perspectives in medicinal chemistry: Metalloprotein inhibitors: What Have We Made and What is the Next Step? *Curr. Top. Med. Chem.* **2016**, *16*, 467-469.

11. Yang, Y.; Hu, X. Q.; Li, Q. S.; Zhang, X. X.; Ruan, B. F.; Xu, J.; Liao, C. Metalloprotein inhibitors for the treatment of human diseases. *Curr. Top. Med. Chem.* **2016**, *16*, 384-396.

12. Jacobsen, J.; Fullagar, J.; Miller, M.; Cohen, S. Identifying chelators for metalloprotein inhibitors using a fragment-based approach. *J. Med. Chem.* **2011**, *54*, 591-602.

13. Dupont, C. L.; Yang, S.; Palenik, B.; Bourne, P. E. Modern proteomes contain putative imprints of ancient shifts in trace metal geochemistry. *Proc. Natl. Acad. Sci. U. S. A.* **2006**, *103*, 17822-17827.

14. Kawai, K.; Nagata, N. Metal-ligand interactions: an analysis of zinc binding groups using the Protein Data Bank. *Eur. J. Med. Chem.* **2012**, *51*, 271-276.

15. Scott, D. E.; Coyne, A. G.; Hudson, S. A.; Abell, C. Fragment-based approaches in drug discovery and chemical biology. *Biochemistry* **2012**, *51*, 4990−5003.

16. Erlanson, D. A.; Fesik, S. W.; Hubbard, R. E.; Jahnke, W.; Jhoti, H. Twenty years on: the impact of fragments on drug discovery. *Nat. Rev. Drug Discovery* **2016**, *15*, 605-619.

17. Agrawal, A.; Johnson, S. L.; Jacobsen, J. A.; Miller, M. T.; Chen, L.-H.; Pellecchia, M.; Cohen, S. M. Chelator fragment libraries for targeting metalloproteinases. *ChemMedChem* **2010**, *5*, 195–199.

18. Credille, C. V.; Chen, Y.; Cohen, S. M. Fragment-based identification of influenza endonuclease inhibitors. *J. Med. Chem.* **2016**, *59*, 6444-6454.

19. Wischeler, J.; Innocenti, A.; Vullo, D.; Agrawal, A.; Cohen, S.; Heine, A.; Supuran, C.; Klebe, G. Bidentate zinc chelators for α-carbonic anhydrases that produce a trigonal bipyramidal coordination geometry. *ChemMedChem* **2010**, *5*, 1609 – 1615.

20. Maresca, A.; Temperini, C.; Vu, H.; Pham, N. B.; Poulsen, S.-A.; Scozzafava, A.; Quinn, R. J.; Supuran, C. T. Non-zinc mediated inhibition of carbonic anhydrases: Coumarins are a new class of suicide inhibitors. *J. Am. Chem. Soc.* **2009**, *131*, 3057-3062.

21. Davis, R. A.; Vullo, D.; Maresca, A.; Supuran, C. T.; Poulsen, S.-A. Natural product coumarins that inhibit human carbonic anhydrases. *Bioorg. Med. Chem.* **2013**, *21*, 1539-1543.

22. Moeker, J.; Peat, T. S.; Bornaghi, L. F.; Vullo, D.; Supuran, C. T.; Poulsen, S.-A. Cyclic secondary sulfonamides: Unusually good inhibitors of cancer-related carbonic anhydrase enzymes. *J. Med. Chem.* **2014**, *57*, 3522-3531.

23. Poulsen, S.-A. Direct screening of a dynamic combinatorial library using mass spectrometry. *J. Am. Soc. Mass Spectrom.* **2006**, *17*, 1074-1080.

24. Kopecka, J.; Rankin, G. M.; Salaroglio, I. C.; Poulsen, S. A.; Riganti, C. P-glycoprotein-mediated chemoresistance is reversed by carbonic anhydrase XII inhibitors. *Oncotarget* **2016**, *7*, 85861-85875.

25. Supuran, C. T. Carbonic anhydrases: novel therapeutic applications for inhibitors and activators. *Nat. Rev. Drug Discovery* **2008**, *7*, 168-181.

26. Parks, S. K.; Cormerais, Y.; Durivault, J.; Pouyssegur, J. Genetic disruption of the pHi-regulating proteins Na+/H+ exchanger 1 (SLC9A1) and carbonic anhydrase 9 severely reduces growth of colon cancer cells. *Oncotarget* **2017**, *8*, 10225-10237.

27. Poulsen, S. Carbonic anhydrase inhibition as a cancer therapy: a review of patent literature, 2007-2009. *Expert Opin. Ther. Patents* **2010**, *20*, 795-806.

28. Mujumdar, P.; Teruya, K.; Tonissen, K.; Vullo, D.; Supuran, C.; Peat, T.; Poulsen, S.-A. An unusual natural product primary sulfonamide: Synthesis, carbonic anhydrase inhibition, and protein X-ray structures of psammaplin C. *J. Med. Chem.* **2016**, *59*, 5462–5470.

29. Woods, L.; Dolezal, O.; Ren, B.; Ryan, J.; Peat, T.; Poulsen, S. Native state mass spectrometry, Surface plasmon resonance, and X-ray crystallography correlate strongly as a fragment screening combination. *J. Med. Chem.* **2016**, *59*, 2192–2204.

30. Ryde, U. Carboxylate binding modes in zinc proteins: a theoretical study. *Biophys. J.* **1999**, *77*, 2777-2787.

31. Jacobsen, J. A.; Major Jourden, J. L.; Miller, M. T.; Cohen, S. M. To bind zinc or not to bind zinc: an examination of innovative approaches to improved metalloproteinase inhibition. *Biochim. Biophys. Acta* **2010**, *1803*, 72-94.

32. Liang, J.; Lipscomb, W. N. Binding of sulfonamide and acetamide to the active-site Zn2+ in carbonic anhydrase: a theoretical study. *Biochemistry* **1989**, *28*, 9724-9733.

33. Boriack, P. A.; Christianson, D. W.; Kingery-Wood, J.; Whitesides, G. M. Secondary interactions significantly removed from the sulfonamide binding pocket of carbonic anhydrase II influence inhibitor binding constants. *J. Med. Chem.* **1995**, *38*, 2286-2291.

34. Martin, D.; Hann, Z.; Cohen, S. Metalloprotein–inhibitor binding: Human carbonic anhydrase II as a model for probing metal–ligand interactions in a metalloprotein active site. *Inorganic Chemistry* **2013**, *52*, 12207–12215.

35. Swayze, E. E.; Jefferson, E. A.; Sannes-Lowery, K. A.; Blyn, L. B.; Risen, L. M.; Arakawa, S.; Osgood, S. A.; Hofstadler, S. A.; Griffey, R. H. SAR by MS: a ligand based technique for drug lead discovery against structured RNA targets. *J. Med. Chem.* **2002**, *45*, 3816-3819.

36. Alterio, V.; Di Fiore, A.; D'Ambrosio, K.; Supuran, C. T.; De Simone, G. Multiple binding modes of inhibitors to carbonic anhydrases: How to design specific drugs targeting 15 different isoforms? *Chem. Rev.* **2012**, *112*, 4421-4468.

36a. Hopkins, A. L.; Groom, C. R.; Alex, A. Ligand efficiency: a useful metric for lead selection. *Drug Discov* Today **2004**, *9*, 430-431.

36b. Daina, A.; Michielin, O.; Zoete, V. SwissADME: a free web tool to evaluate pharmacokinetics, drug-likeness and medicinal chemistry friendliness of small molecules. *Sci. Rep.* **2017**, *7*, 42717, doi: 10.1038/srep42717.

37. Lipinski, C.; Fiese, E. F.; Korst, R. J. pKa, Log P and MedChem CLOGP fragment values of acidic heterocyclic potential bioisosteres. *Quant. Struct.-Act. Relat.* **1991**, *10*, 109-117.

38. Liu, W.; Lau, F.; Liu, K.; Wood, H. B.; Zhou, G.; Chen, Y.; Li, Y.; Akiyama, T. E.; Castriota, G.; Einstein, M.; Wang, C.; McCann, M. E.; Doebber, T. W.; Wu, M.; Chang, C. H.; McNamara, L.; McKeever, B.; Mosley, R. T.; Berger, J. P.; Meinke, P. T. Benzimidazolones: A new class of selective peroxisome proliferator activated receptor γ (PPARγ) modulators. *J. Med. Chem.* **2011**, *54*, 8541−8554.

39. Hofstadler, S. A.; Sannes-Lowery, K. A. Applications of ESI-MS in drug discovery: interrogation of noncovalent complexes. *Nat. Rev. Drug Discovery* **2006**, *5*, 585-595.

40. (a) Leney, A. C.; Heck, A. J. R. Native mass spectrometry: What is in the name? *J. Am. Soc. Mass Spectrom.* **2017**, *28*, 5-13. (b) Kitova, E. N.; El-Hawiet, A.; Schnier, P. D.; Klassen, J. S. Reliable determinations of protein–ligand interactions by direct ESI-MS measurements. Are we there yet*? J. Am. Soc. Mass Spectrom.* **2012**, *23*, 431–441. (c) Zhang, S.; Van Pelt, C. K.; Wilson, D. B. Quantitative setermination of noncovalent binding interactions using automated nanoelectrospray mass spectrometry. *Anal. Chem.* **2003**, *75*, 3010-3018.

41. Vivat-Hannah, V.; Atmanene, C.; Zeyer, D.; Van Dorsselaer, A.; Sanglier-Cianférani, S. Native MS: an 'ESI, way to support structure - and fragment-based drug discovery. *Future Med. Chem.* **2010**, *2*, 35-50.

42. Maple, H. J.; Garlish, R. A.; Rigau-Roca, L.; Porter, J.; Whitcombe, I.; Prosser, C. E.; Kennedy, J.; Henry, A. j.; Taylor, R. J.; Crump, M. P.; Crosby, J. Automated protein−ligand interaction screening by mass spectrometry. *J. Med. Chem.* **2012**, *55*, 837-851.

43. Drinkwater, N.; Vu, H.; Lovell, K. M.; Criscione, K. R.; Collins, B. M.; Prisinzano, T. E.; Poulsen, S.-A.; McLeish, M. J.; Grunewald, G. L.; Martin, J. L. Fragment-based screening by X-ray crystallography, MS and isothermal titration calorimetry to identify PNMT (phenylethanolamine N-methyltransferase) inhibitors *Biochem. J.* **2010**, *431*, 51-61.

44. Poulsen, S.-A. Fragment screening by native state mass spectrometry. *Aust. J. Chem.* **2013**, *66*, 1495–1501.

45. Pedro, L.; Quinn, R. J. Native mass spectrometry in fragment-based drug discovery. *Molecules* **2016**, *21*, 984-999.

46. Hulme, E. C.; Trevethick, M. A. Ligand binding assays at equilibrium: validation and interpretation. *Br. J. Pharmacol.* **2010**, *161*, 1219-1237.

46a. Schiebel, J.; Radeva, N.; Koster, H.; Metz, A.; Krotzky, T.; Kuhnert, M.; Diederich, W. E.; Heine, A.; Neumann, L.; Atmanene, C.; Roecklin, D.; Vivat-Hannah, V.; Renaud, J.-P.; Meinecke, R.; Schlinck, N.; Sitte, A.; Popp, F.; Zeeb, M.; Klebe, G. One question, multiple answers: biochemical and biophysical screening methods retrieve deviating fragment hit lists. *ChemMedChem* **2015**, 10, 1511-1521.

47. Ermolenko, L.; Zhaoyu, H.; Lejeune, C.; Vergne, C.; Ratinaud, C.; Nguyen, T. B.; Al-Mourabit, A. Concise synthesis of Didebromohamacanthin A and Demethylaplysinopsine: addition of ethylenediamine and guanidine derivatives to the pyrrole-amino acid diketopiperazines in oxidative conditions. *Org. Lett.* **2014**, *16*, 872-875.

48. Baell, J. B.; Holloway, G. A. New Substructure Filters for Removal of Pan Assay Interference Compounds (PAINS) from Screening Libraries and for Their Exclusion in Bioassays. *J. Med. Chem.* **2010**, *53*, 2719-2740.

49. Oikonomakos, N. G., Skamnaki, V.T., Osz, E., Szilagyi, L., Somsak, L., Docsa, T., Toth, B., Gergely, P. Kinetic and crystallographic studies of glucopyranosylidene spirothiohydantoin binding to glycogen phosphorylase B. *Bioorg. Med. Chem.* **2002**, *10*, 261-268.

50. Zidar, N.; Tomasic, T.; Sink, R.; Rupnik, V.; Kovac, A.; Turk, S.; Patin, D.; Blanot, D.; Contreras Martel, C.; Dessen, A.; Muller Premru, M.; Zega, A.; Gobec, S.; Peterlin Masic, L.; Kikelj, D. Discovery of novel 5-benzylidenerhodanine and 5-benzylidenethiazolidine-2,4-dione inhibitors of MurD ligase. *J. Med. Chem.* **2010**, *53*, 6584-6594.

51. Tomasic, T.; Zidar, N.; Sink, R.; Kovac, A.; Blanot, D.; Contreras-Martel, C.; Dessen, A.; Muller-Premru, M.; Zega, A.; Gobec, S.; Kikelj, D.; Masic, L. P. Structure-based design of a new series of D-glutamic acid based inhibitors of bacterial UDP-N-acetylmuramoyl-L-alanine:D-glutamate ligase (MurD). *J. Med. Chem.* **2011**, *54*, 4600-4610.

52. Tomasic, T., Sink, R., Zidar, N., Fic, A., Contreras-Martel, C., Dessen, A., Patten, D., Blanot, D., Muller-Premru, M., Gobec, S., Zega, A., Kikelj, D., and Masic, L. P. . Dual inhibitor of MurD and MurE ligases from Escherichia coli and staphylococcus aureus. *ACSMed.Chem.Lett.* **2012**, *3*, 626-630.

53. Nolte, R. T.; Wisely, G. B.; Westin, S.; Cobb, J. E.; Lambert, M. H.; Kurokawa, R.; Rosenfeld, M. G.; Willson, T. M.; Glass, C. K.; Milburn, M. V. Ligand binding and co-activator assembly of the peroxisome proliferator-activated receptor-gamma. *Nature* **1998**, *395*, 137-143.

54. Binda, C.; Aldeco, M.; Geldenhuys, W. J.; Tortorici, M.; Mattevi, A.; Edmondson, D. E. Molecular insights into Human monoamine oxidase B inhibition by the Glitazone anti-diabetes drugs. *ACS Med. Chem. Lett.* **2011**, *3*, 39-42.

55. Good, A. C.; Liu, J.; Hirth, B.; Asmussen, G.; Xiang, Y.; Biemann, H. P.; Bishop, K. A.; Fremgen, T.; Fitzgerald, M.; Gladysheva, T.; Jain, A.; Jancsics, K.; Metz, M.; Papoulis, A.; Skerlj, R.; Stepp, J. D.; Wei, R. R. Implications of promiscuous Pim-1 kinase fragment inhibitor hydrophobic interactions for fragment-based drug design. *J. Med. Chem.* **2012**, *55*, 2641-2648.

56. Hughes, S. J.; Millan, D. S.; Kilty, I. C.; Lewthwaite, R. A.; Mathias, J. P.; O'Reilly, M. A.; Pannifer, A.; Phelan, A.; Stuhmeier, F.; Baldock, D. A.; Brown, D. G. Fragment based discovery of a novel and selective PI3 kinase inhibitor. *Bioorg. Med. Chem. Lett.* **2011**, *21*, 6586-6590.

57. Dakin, L. A.; Block, M. H.; Chen, H.; Code, E.; Dowling, J. E.; Feng, X.; Ferguson, A. D.; Green, I.; Hird, A. W.; Howard, T.; Keeton, E. K.; Lamb, M. L.; Lyne, P. D.; Pollard, H.; Read, J.; Wu, A. J.; Zhang, T.; Zheng, X. Discovery of novel benzylidene-1,3-thiazolidine-2,4-diones as potent and selective inhibitors of the PIM-1, PIM-2, and PIM-3 protein kinases. *Bioorg. Med. Chem. Lett.* **2012**, *22*, 4599-4604.

58. Camps, M.; Ruckle, T.; Ji, H.; Ardissone, V.; Rintelen, F.; Shaw, J.; Ferrandi, C.; Chabert, C.; Gillieron, C.; Francon, B.; Martin, T.; Gretener, D.; Perrin, D.; Leroy, D.; Vitte, P. A.; Hirsch, E.; Wymann, M. P.; Cirillo, R.; Schwarz, M. K.; Rommel, C. Blockade of PI3Kgamma suppresses joint inflammation and damage in mouse models of rheumatoid arthritis. *Nature Medicine* **2005**, *11*, 936-943.

59. Richardson, C. M.; Nunns, C. L.; Williamson, D. S.; Parratt, M. J.; Dokurno, P.; Howes, R.; Borgognoni, J.; Drysdale, M. J.; Finch, H.; Hubbard, R. E.; Jackson, P. S.; Kierstan, P.; Lentzen, G.; Moore, J. D.; Murray, J. B.; Simmonite, H.; Surgenor, A. E.;

Torrance, C. J. Discovery of a potent CDK2 inhibitor with a novel binding mode, using virtual screening and initial, structure-guided lead scoping. *Bioorg. Med. Chem. Lett.* **2007**, *17*, 3880-3885.

60. Zidar, N.; Tomasic, T.; Sink, R.; Kovac, A.; Patin, D.; Blanot, D.; Contreras-Martel, C.; Dessen, A.; Premru, M. M.; Zega, A.; Gobec, S.; Masic, L. P.; Kikelj, D. New 5-benzylidenethiazolidin-4-one inhibitors of bacterial MurD ligase: design, synthesis, crystal structures, and biological evaluation. *Eur. J. Med. Chem.* **2011**, *46*, 5512-5523.

61. Gillilan, R. E.; Ayers, S. D.; Noy, N. Structural basis for activation of fatty acid-binding protein 4. *J. Mol. Biol.* **2007**, *372*, 1246-1260.

62. Yu, W.; Guo, Z.; Orth, P.; Madison, V.; Chen, L.; Dai, C.; Feltz, R. J.; Girijavallabhan, V. M.; Kim, S. H.; Kozlowski, J. A.; Lavey, B. J.; Li, D.; Lundell, D.; Niu, X.; Piwinski, J. J.; Popovici-Muller, J.; Rizvi, R.; Rosner, K. E.; Shankar, B. B.; Shih, N.-Y.; Arshad Siddiqui, M.; Sun, J.; Tong, L.; Umland, S.; Wong, M. K. C.; Yang, D.-y.; Zhou, G. Discovery and SAR of hydantoin TACE inhibitors. *Bioorg. Med. Chem. Lett.* **2010**, *20*, 1877-1880.

63. Yu, W.; Tong, L.; Kim, S. H.; Wong, M. K.; Chen, L.; Yang, D. Y.; Shankar, B. B.; Lavey, B. J.; Zhou, G.; Kosinski, A.; Rizvi, R.; Li, D.; Feltz, R. J.; Piwinski, J. J.; Rosner, K. E.; Shih, N. Y.; Siddiqui, M. A.; Guo, Z.; Orth, P.; Shah, H.; Sun, J.; Umland, S.; Lundell, D. J.; Niu, X.; Kozlowski, J. A. Biaryl substituted hydantoin compounds as TACE inhibitors. *Bioorg. Med. Chem. Lett.* **2010**, *20*, 5286-5289.

64. Durham, T. B.; Klimkowski, V. J.; Rito, C. J.; Marimuthu, J.; Toth, J. L.; Liu, C.; Durbin, J. D.; Stout, S. L.; Adams, L.; Swearingen, C.; Lin, C.; Chambers, M. G.; Thirunavukkarasu, K.; Wiley, M. R. Identification of potent and selective hydantoin inhibitors of aggrecanase-1 and aggrecanase-2 that are efficacious in both chemical and surgical models of osteoarthritis. *J. Med. Chem.* **2014**, *57*, 10476-10485.

65. De Savi, C.; Waterson, D.; Pape, A.; Lamont, S.; Hadley, E.; Mills, M.; Page, K. M.; Bowyer, J.; Maciewicz, R. A. Hydantoin based inhibitors of MMP13--discovery of AZD6605. *Bioorg. Med. Chem. Lett.* **2013**, *23*, 4705-4712.

66. Francesco, I. N.; Wagner, A.; Colobert, F. Suzuki–Miyaura coupling reaction of boronic acids and ethyl glyoxylate: Synthetic access to mandelate derivatives. *Eur. J. Org. Chem.* **2008**, 5692-5695.

67. Sheehan, J. C.; Laubach, G. D. The Synthesis of Substituted Penicillins and Simpler Structural Analogs. V. The Application of 5-Phenyloxazolidine-2,4-diones to the Synthesis of Phenylacetylamino-β-lactams. *J. Am. Chem. Soc.* **1951**, *73*, 4752-4755.

68. Al-Horani, R. A.; Desai, U. R. Electronically rich N-substituted tetrahydroisoquinoline 3-carboxylic acid esters: concise synthesis and conformational studies. *Tetrahedron* **2012**, *68*, 2027-2040.

69. Tang, S. Q.; Lee, Y. Y. I.; Packiaraj, D. S.; Ho, H. K.; Chai, C. L. L. Systematic Evaluation of the metabolism and toxicity of thiazolidinone and imidazolidinone heterocycles. *Chem. Res. Toxicol.* **2015**, *28*, 2019-2033.

70. Kottakota, S. K.; Benton, M.; Evangelopoulos, D.; Guzman, J. D.; Bhakta, S.; McHugh, T. D.; Gray, M.; Groundwater, P. W.; Marrs, E. C. L.; Perry, J. D.; Harburn, J. J. Versatile routes to marine sponge metabolites through benzylidene rhodanines. *Org. Lett.* **2012**, *14*, 6310-6313.

71. Giles, R. G.; Lewis, N. J.; Quick, J. K.; Sasse, M. J.; Urquhart, M. W. J.; Youssef, L. Regiospecific reduction of 5-benzylidene-2,4-thiazolidinediones and 4-oxo-2-thiazolidinethiones using lithium borohydride in pyridine and tetrahydrofuran. *Tetrahedron* **2000**, *56*, 4531-4537.

72. Willot, M.; Chen, J. C.; Zhu, J. Combination of lithium Ccloride and hexafluoroisopropanol for Friedel-Crafts reactions. *Syn. Lett.* **2009**, 577-580.

73. Goutelle, S.; Maurin, M.; Rougier, F.; Barbaut, X.; Bourguignon, L.; Ducher, M.; Maire, P. The Hill equation: a review of its capabilities in pharmacological modelling. *Fundam. Clin. Pharmacol.* **2008**, *22*, 633-648.

74. Papalia, G. A.; Leavitt, S.; Bynum, M. A.; Katsamba, P. S.; Wilton, R.; Qiu, H.; Steukers, M.; Wang, S.; Bindu, L.; Phogat, S.; Giannetti, A. M.; Ryan, T. E.; Pudlak, V. A.; Matusiewicz, K.; Michelson, K. M.; Nowakowski, A.; Pham-Baginski, A.; Brooks, J.; Tieman, B. C.; Bruce, B. D.; Vaughn, M.; Baksh, M.; Cho, Y. H.; deWit, M.; Smets, A.; Vandersmissen, J.; Michiels, L.; Myszka, D. G. Comparative analysis of 10 small molecules binding to carbonic anhydrase II by different investigators using Biacore technology. *Anal. Biochem.* **2006**, *359*, 94−105.

75. Kabsch, W. XDS. *Acta Crystallogr. Sect. D: Biol. Crystallogr.* **2010**, *66*, 125-132.

76. Evans, P. R. An introduction to data reduction: space-group determination, scaling and intensity statistics. *Acta Crystallogr. D Biol. Crystallogr.* **2011**, *67*, 282-292.

77. McCoy, A. J.; Grosse-Kunstleve, R. W.; Adams, P. D.; Winn, M. D.; Storoni, L. C.; Read, R. J. Phaser crystallographic software. *J. Appl. Crystallogr.* **2007**, *40*, 658-674.

78. Emsley, P.; Lohkamp, B.; Scott, W. G.; Cowtan, K. Features and development of Coot. *Acta Crystallogr. D Biol. Crystallogr.* **2010**, *66*, 486-501.

79. Murshudov, G. N.; Skubak, P.; Lebedev, A. A.; Pannu, N. S.; Steiner, R. A.; Nicholls, R. A.; Winn, M. D.; Long, F.; Vagin, A. A. REFMAC5 for the refinement of macromolecular crystal structures. *Acta Crystallogr. D Biol. Crystallogr.* **2011**, *67*, 355-367.

80. Afonine, P. V.; Grosse-Kunstleve, R. W.; Echols, N.; Headd, J. J.; Moriarty, N. W.; Mustyakimov, M.; Terwilliger, T. C.; Urzhumtsev, A.; Zwart, P. H.; Adams, P. D. Towards automated crystallographic structure refinement with phenix.refine. *Acta Crystallogr. D Biol. Crystallogr.* **2012**, *68*, 352-367.

81. Moriarty, N. W.; Grosse-Kunstleve, R. W.; Adams, P. D. Electronic Ligand Builder and Optimization Workbench (eLBOW): a tool for ligand coordinate and restraint generation. *Acta Crystallogr. D* **2009**, *65*, 1074-1080.

Table of Contents Graphic